Calhoun: The NPS Institutional Archive

DSpace Repository

Theses and Dissertations 1. Thesis and Dissertation Collection, all items

1971

# An investigation of subsonic diffuser performance.

Sharer, Kevin Woods

Monterey, California ; Naval Postgraduate School

http://hdl.handle.net/10945/15782

*Downloaded from NPS Archive: Calhoun*

Calhoun is the Naval Postgraduate School's public access digital repository for research materials and institutional publications created by the NPS community. Calhoun is named for Professor of Mathematics Guy K. Calhoun, NPS's first appointed -- and published -- scholarly author.

Dudley Knox Library / Naval Postgraduate School
411 Dyer Road / 1 University Circle
Monterey, California USA 93943

http://www.nps.edu/library

# AN INVESTIGATION OF SUBSONIC DIFFUSER PERFORMANCE

Kevin Woods Sharer

United States
Naval Postgraduate School

# THESIS

## AN INVESTIGATION OF SUBSONIC DIFFUSER PERFORMANCE

by

Kevin Woods Sharer

Thesis Advisor: Kyriacos Papailiou

June 1971

*Approved for public release; distribution unlimited.*

T139917

# An Investigation of Subsonic Diffuser Performance

by

Kevin Woods Sharer
Ensign, United States Navy
B.S.A.E., United States Naval Academy, 1970

Submitted in partial fulfillment of the
requirements for the degree of

MASTER OF SCIENCE IN AERONAUTICAL ENGINEERING

from the

NAVAL POSTGRADUATE SCHOOL
June 1971

# ABSTRACT

This report investigates subsonic diffuser performance, with emphasis on conical and annular geometries. A correlation is presented which aids in the prediction of performance. Two annular diffusers were designed and tested to help substantiate the correlation.

# TABLE OF CONTENTS

LIST OF ILLUSTRATIONS 4

LIST OF SYMBOLS 6

ACKNOWLEDGEMENT 8

I. INTRODUCTION 9

  A. GENERAL DESCRIPTION OF THE FLOW 9

  B. REVIEW OF PREVIOUS WORK 13

II. DERIVATION OF THE SHAPE PARAMETER OMEGA 17

III. ORIGINAL SUGGESTION FOR THE USE OF OMEGA 28

IV. AN ALTERNATE DERIVATION OF OMEGA 33

  A. CONICAL 34

  B. TWO DIMENSIONAL 35

  C. ANNULAR 35

V. PARAMETER STUDY 39

VI. DATA CORRELATIONS 44

VII. EXPERIMENTAL WORK 56

  A. EXPERIMENTAL EQUIPMENT 56

  B. EXPERIMENTAL RESULTS 58

VIII. CONCLUSIONS AND RECOMMENDATIONS 68

APPENDIX A - List of Programs 69

BIBLIOGRAPHY 78

INITIAL DISTRIBUTION LIST 79

FORM DD 1473 80

# LIST OF ILLUSTRATIONS

| Figure | | Page |
|---|---|---|
| 1 | Diffuser Geometries | 15 |
| 2 | Differential flow element | 25 |
| 2(a,b) | Annular Channel Sections | 26 |
| 3 | T-s diagram for an adiabatic compression | 27 |
| 4 | Vavra's plot of some 2-D data | 30 |
| 5 | Gapp's plot of reference 6 data | 31 |
| 6 | Flow regimes of reference 5 | 32 |
| 7 | Inlet section | 38 |
| 8 | Constant $\Omega$ lines for a conical diffuser | 42 |
| 9 | Constant $\Omega$ lines for an annular diffuser with a given inlet geometry | 43 |
| 10 | Constant area ratio plot | 49 |
| 11 | $\Omega, \bar{C}_f$ vs. $A^{\cdot}(x)/\Delta R$ | 50 |
| 12(a) | List of symbols | 51 |
| 12 | $L/\Delta R$ vs. $\Omega C_f \Delta R/[A^{\cdot}(x) - 1.5]$ | 52 |
| 13 | $L/\Delta R$ vs. $\Omega C_f (\Delta R)^2/A^{\cdot}(x)^2$ | 53 |
| 14 | $C_f$ vs. PAR 4 | 54 |
| 15 | $C_P/\Omega$ vs. PAR4 | 55 |
| 16 | Model schematic | 60 |
| 17 | Inner body and model two | 61 |
| 18 | Contraction cone and model one | 61 |
| 19 | Overall drawing of apparatus | 62 |
| 20 | Photograph of equipment | 63 |
| 21 | Contraction cone velocity profile | 64 |

Figure Page

22 Velocity profile at inlet of model 2 65

23 Model one performance 66

24 Model two performance 67

# LIST OF SYMBOLS

| Symbol | Definition | Units |
|---|---|---|
| $A$ | Area | $ft^2$ |
| $A'(X)$ | Area Gradient | ft |
| $C$ | Wetted perimeter | ft |
| $C_p$ | Coefficient of pressure recovery | -- |
| $C_{pi}$ | Ideal pressure recovery coefficient | -- |
| $C_f$ | Average coefficient of friction | -- |
| $C_p$ | Specific heat of air | $BTU/lbm\text{-}^{o}R$ |
| $\Delta R$ | Inlet radius difference | in. |
| $g_c$ | Acceleration of gravity | $ft\text{-}lb_m/lb\text{-}sec^2$ |
| $L$ | Axial length | in. |
| $\dot{m}$ | Mass flow rate | lbm/sec |
| $\dot{m}_{1r}$ | Referred mass flow rate | -- |
| $n$ | Polytropic exponent | -- |
| $P$ | Total pressure | $lb/in^2$ |
| $P$ | Static pressure | $lb/in^2$ |
| $q$ | Dynamic pressure $(P_t - P)$ | $lb/in^2$ |
| RT1 | Inlet outer radius | in |
| RH1 | Inlet inner radius | in |
| $T_t$ | Total temperature | $^{o}R$ |
| $T$ | Static temperature | $^{o}R$ |
| $\Theta_i$ | Inner wall angle | -- |
| $\Theta_o$ | Outer wall angle | -- |
| $\Theta$ | Wall angle for conical case | -- |
| $\Omega$ | Shape parameter | -- |

| Symbol | Definition | Units |
|---|---|---|
| PAR4C | Quotient of the ideal recovery coefficient and omega for the conical case | -- |
| PAR4A | Quotient of the ideal recovery coefficient and omega for the annular case | -- |
| PAR4 | The general symbol for the quotient of the ideal recovery coefficient and omega which encompasses both PAR4C and PAR4A | -- |

Subscripts

| | |
|---|---|
| 1 | Diffuser inlet station |
| is | Isentropic |
| t | Total |

# ACKNOWLEDGEMENT

The author wishes to acknowledge the patience and guidance of Professor K. D. Papailiou of the Naval Postgraduate School in the preparation of the thesis. Without the able assistance of Mr. James Hammer and the creative skill of the model maker, Mr. Gordon Gulbranson, the experimental portion of the thesis would not have been possible.

# I. INTRODUCTION

The diffuser is a device used in fluid mechanical systems to convert kinetic energy into static pressure by decelerating the flow. There are several basic straight-walled diffuser shapes such as conical, two dimensional and annular as shown in Figure 1. Much attention has been given to two dimensional diffusers and several successful correlations have been developed, but annular and conical diffusers have not been as exhaustively studied and good new correlations would be very useful to the designer.

## A. A GENERAL DESCRIPTION OF THE FLOW

A diffuser should convert kinetic energy of the flow into pressure with a minimum of losses due to viscous effects. Also it is desirable to make optimum use of the geometric area ratio, because the area ratio prescribes the amount of diffusion that is possible under ideal conditions. Bernoulli's equation relates the total fluid energy to the static pressure and kinetic energy; and if the flow experiences no losses due to friction or other non isentropic processes the total energy of the fluid remains constant. Any decrease in velocity will cause the static pressure to rise, so that in an ideal diffuser all kinetic energy losses show up as pressure gains. Unfortunately, most fluids experience losses, and the goal of any flow analysis is to keep track of the fluid energy whether it is dissipated or converted from flow energy into static pressure. Dissipation of kinetic energy takes

place inside the boundary layers where large velocity gradients exist so that the viscous effects become important.

The boundary layer is a thin region adjacent to the wall in which the velocity increases from zero to the free stream value. Since the fluid in the boundary layer is moving slower than that in the free stream, it does not have as much kinetic energy as the bulk of the flow. The transverse velocity gradients that are present give rise to shear stresses which are related to the velocity gradients through the coefficient of viscosity for laminar flow. In a turbulent boundary layer the shear stresses are not related to the gradients in such a simple fashion. However, it is possible to model turbulent flow as an average motion plus time dependent fluctuations whose average value is zero. When the boundary layer equations are modified for turbulent flows, additional shear stress terms are present known as Reynolds stresses. These Reynolds stresses are in fact the predominant stresses for a turbulent boundary layer.

Since the flow in diffusers is constantly decelerating, due to increasing area, the flow faces an increasing pressure as it traverses the channel. To overcome the increasing pressure the flow must transform kinetic energy into pressure. However, as mentioned the flow in the boundary layer is not as energetic as the free stream, but it feels the same longitudinal pressure gradient. When the fluid near the wall does not have the energy to overcome the pressure rise, the flow higher up in the boundary layer must pull it along by shearing action. In this sense the turbulent boundary layer is more capable of meeting an adverse

pressure gradient than a laminar one because of the additional Reynolds stresses. For this reason it is advantageous for diffusing flows to be turbulent in order to withstand the decelerations imposed in a diffuser. A point is reached, however; where the outer layers can no longer pull the inner layers, and the flow is forced away from the wall and separation results. Large scale separation with recirculating flow causes intolerable losses in a diffuser and is to be avoided. Any time the boundary layer does not have sufficient energy to overcome the pressure gradient it will separate, so it is necessary to find out something about the way the pressure gradient behaves in a diverging channel.

Bernoulli's equation is written as follows

$$P_t = P + \frac{1}{2} \rho V^2 \qquad (1)$$

Since the boundary layer feels the same pressure distribution as the free stream, it is only necessary to calculate the free stream pressure distribution which shall be calculated here assuming inviscid one dimensional flow in the core. Taking the derivitive of (1) gives

$$dp/dx = -V\,dV/dx \qquad (2)$$

with continuity and constant density

$$\dot{m} = \rho A V = \rho_1 A_1 V_1 \qquad (3)$$

or

$$dA/A = -dV/V \quad \text{OR} \quad V\,dV = (-V^2/A)\,dA \qquad (4)$$

replacing (4) in (2)

$$dp/dx = (-\rho V^2/A)\, dA/dx \qquad (5)$$

with continuity

$$dp/dx = (\rho A_1^2 V_1^2/A^2)\, dA/dx \qquad (6)$$

or

$$d(p/\tfrac{1}{2}\rho V^2)/dx = d(p/q)/dx = (2A_1^2/A^3)\, dA/dx \qquad (7)$$

(7) shows that the pressure gradient is the strongest at the inlet of a diffuser since the area gradient, $dA/dx$, is very nearly constant for a given straight walled diffuser. This is compatible with the state of the boundary layer which is "young" at the entrance of the diffuser and is able to overcome large pressure gradients. The large initial gradient suggests that a boundary layer should be as thin as possible at the entrance to a diffuser for best performance; i.e., avoidance of early separation. This fact has been substantiated by many researchers by increasing the inlet boundary layer thickness and noting a decrease in performance, Kline [Ref. 1]. Returning to the expression for the pressure gradient, (7), it can be seen that the gradient may be high initially. But a large area gradient also insures that the pressure gradient term will decrease rapidly, because the denominator of (7) contains the local area raised to the third power. Although a general description of the flow conditions in a diffuser has been given, the task remains to determine losses due to the factors considered above.

## B. REVIEW OF PREVIOUS WORK

Many attempts over the years have been made to explain and predict the actions of the flow in the diffuser. As the previous section suggests, it is not a simple process. The major stumbling block is that the phenomenon of turbulence is not well understood, and to predict separation the growth of the boundary layer must be calculated. In order to bypass the turbulent flow calculations, more empirical methods and simplifications have been used to predict performance. One of the simpler techniques is that of the equivalent cone angle method as described in Gleason [Ref. 4]. Basically, all flow cross sections are related to an equivalent conical flow with a corresponding wall divergence angle. If the wall divergence angle, which is a direct function of pressure gradient, is below a certain value the diffuser is judged sound. This method is widely used for design but has not always proved adequate. The next level of effort has been directed towards generating performance plots.

After testing a sufficient number of diffusers of a given type, constant pressure recovery lines were plotted on a graph of pertinent geometric parameters such as wall angle versus length. Kline [Ref. 5] has done extensive work in this area for two dimensional diffusers and Sovran and Klomp [Ref. 6] have done the same thing for annular diffusers. Through flow visualization techniques Kline [Ref 5] has been able to generate a plot showing the expected flow regimes for different two dimensional geometries, Figure 6. The line of first stall, a-a, is presented as the optimum performance line, because at or just after this point the boundary layer

has overcome as much of the pressure gradient as possible and is nearing large scale separation or transitory stall. No similar flow regime graphs have been developed for the annular or conical geometries

Several years ago Kline [Ref. 1] developed a more analytic approach to the problem. He has attempted to solve the turbulent equations in predicting performance. The boundary layer and continuity equations have been combined into a mementum integral equation and used with several shear correlations to work up a set of five linear first order differential equations with non linear coefficients. However, the solutions of these equations alone do not predict the performance, a stall criterion is needed. Kline has combined several parameters including boundary layer thickness and rate of area growth into a parameter. When this parameter decreases to a certain value stall is said to occur. The parameter has no physical basis, but it does correlate line a-a of the flow regime chart. In Reference 1 many reports have been analyzed and the criterion in fairly successful for 2D-diffusers. The variation in performance with inlet boundary layer thickness is also demonstrated. Though Kline appears to be fairly successful, the method is rather approximative and requires the solution of a large set of equations. However, Vavra [Ref. 8] has developed a performance parameter which is easy to calculate from geometry and can be derived from basic principles.

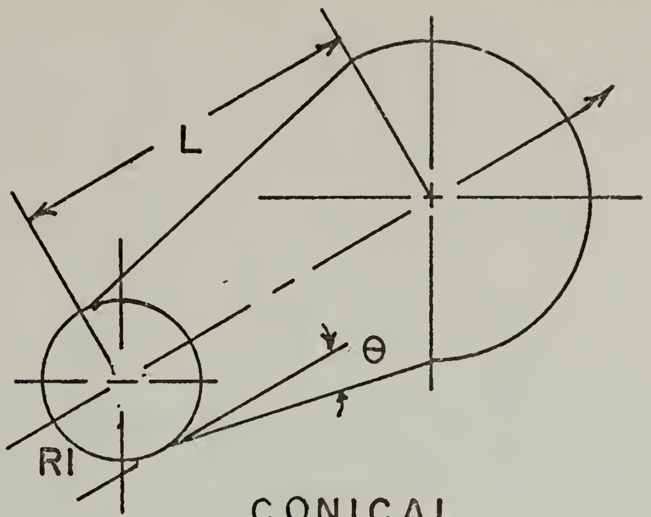

CONICAL

DIFFUSER GEOMETRIES

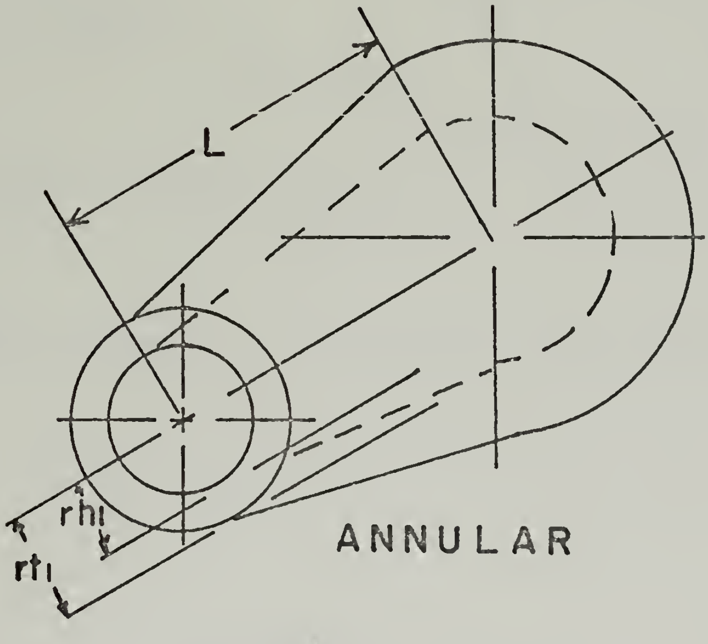

ANNULAR

FIGURE 1

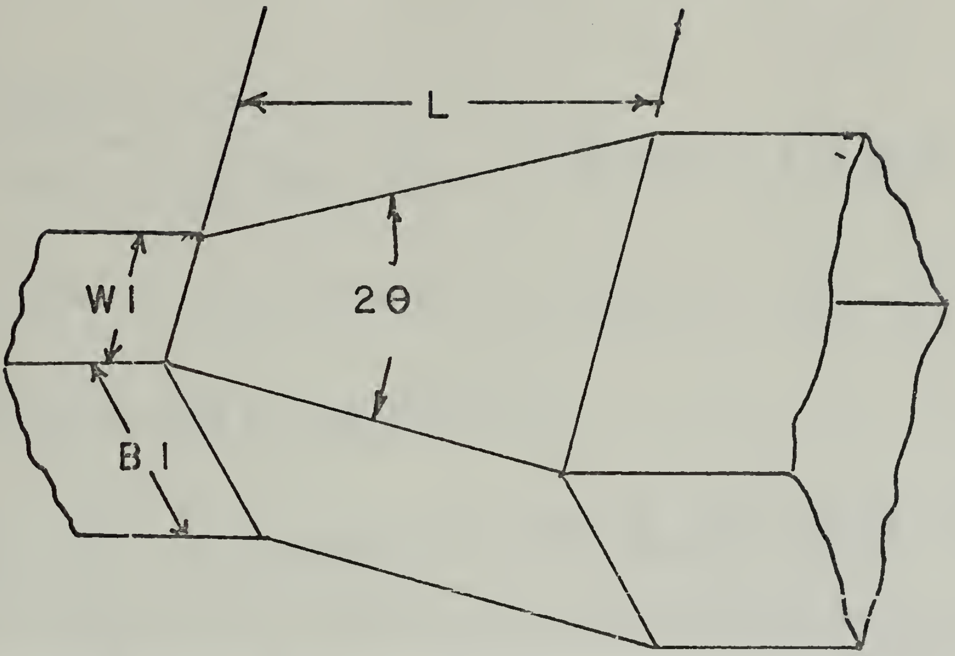

TWO DIMESIONAL

FIGURE 1 (CONCLUDED)

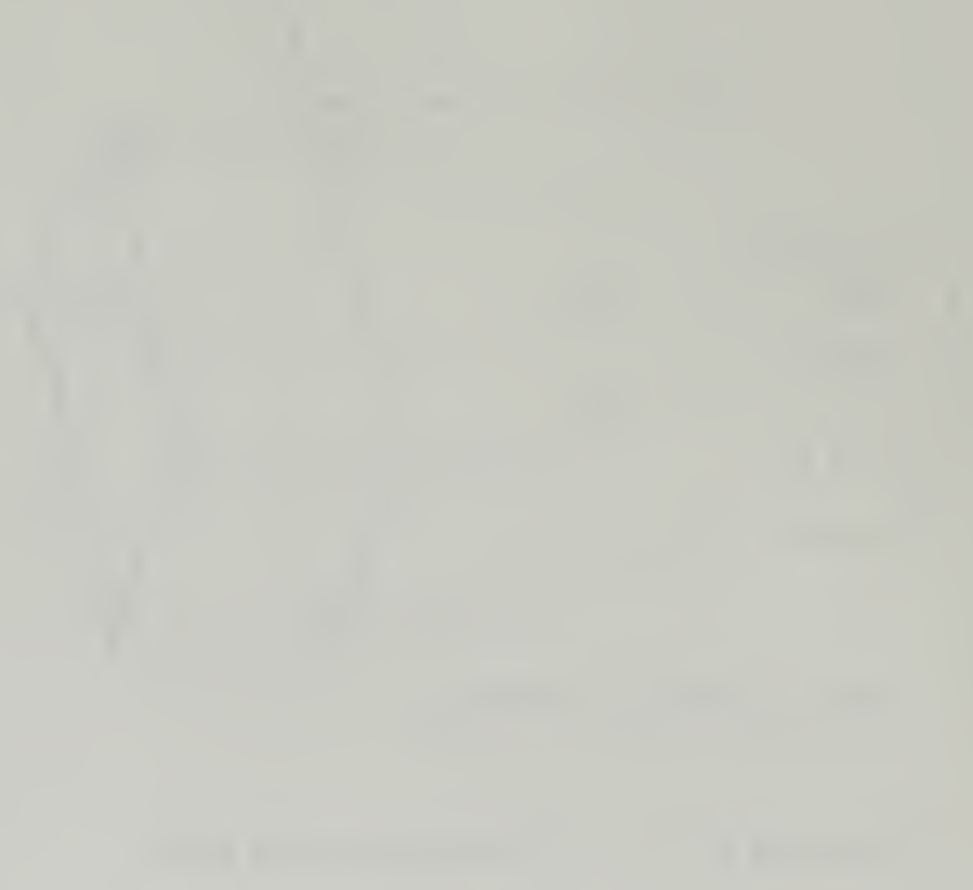

## II. DERIVATION OF THE SHAPE PARAMETER OMEGA

Vavra [Ref. 8] presented the basic derivation, and Gapp [Ref. 3] did a thorough development which is presented below.

The momentum theorum

$$\int_{(S_2)} dm_{s_2}\,\bar{V}_2 - \int_{(S_1)} dm_{s_1}\,\bar{V}_1 = -\int_S \vec{n}\,p\,ds - \int_S \vec{t}\,\tau\,ds \qquad (8)$$

was applied to the differential flow element of Figure 2 to yield

$$(\rho A V)(\bar{V} + d\bar{V}) - (\rho A \bar{V})\,\vec{V} =$$

$$-\vec{n}_1\,pA - \vec{n}_2\,(p+dp)(A+dA) - \vec{n}_3\,p\,dA - \vec{n}_4\,p\,dA - \vec{t}\,\tau C \qquad (9)$$

After expanding and rearranging terms where $\vec{n}_1\,\vec{n}_2\,\vec{n}_3$ and $\vec{n}_4$ are the outward pointing normals of each respective side and $\vec{t}$ is the tangent vector, the theorum gives

$$\rho A V\,dV = -A\,dp - \tau C\,dL \qquad (10)$$

rearranging

$$dp = -\rho V\,dV - \tau c\,dL/A \qquad (11)$$

or

$$d(V^2/2) + dp/\rho = (-\tau/\rho)(C/A)\,dL \qquad (12)$$

Equation (12) may be derived for an annular diffuser as well. From Figure 2 (a) for an annulus

$$dL_1 = dL\cos\gamma \qquad (13)$$

$$A_1 = A/\cos\gamma \qquad (14)$$

From Figure 2 (b)

$$c = 2\pi(r_1 + r_2) = 4\pi r_m \qquad (15)$$

Also $C' = 4\pi r_m$ for small divergences. Replacing (13), (14), and (15) in (12)

$$d(V^2/2) + dp/\rho = (-\tau/\rho)(c'/A_1 \cos\gamma)\, dL_1 \cos\gamma =$$

$$\tau\, c'\, dL_1 / \rho A_1$$

So finally considering only sections normal to the axis and omitting the prime

$$d(V^2/2) + dp/\rho = (-\tau/\rho)(C/A)\, dL$$

as before. From the first law of thermodynamics

$$dQ = du + p\,dv = dh - v\,dp = dh - 1/\rho\, dp = T\,ds \qquad (16)$$

or

$$dp/\rho = dh - T\,ds \qquad (17)$$

Replacing (17) in (12) gives

$$dh + d(V^2/2) - T\,ds = (-\tau/\rho)(C/A)\, dL \qquad (18)$$

combining the enthalpy and velocity derivatives into the total enthalpy form

$$dH = T\,ds - (\tau/\rho)(C/A)\, dL \qquad (19)$$

Since the idealized one dimensional process is adiabatic, with no

energy input through the walls, the total enthalpy is constant and its derivative is zero. Therefore (19) reduces to

$$T\,ds = (\tau/\rho)\,(C/A)\,dL \qquad (20)$$

The shear losses in a turbulent boundary layer are not easily determined, but they do give an indication of overall losses. An average shear stress coefficient was defined for the entire channel to reflect these losses.

$$C_f = \tau_{AV}/\tfrac{1}{2}\rho V^2 \qquad (21)$$

or using continuity

$$\tau_{AV} = (C_f/2)\;\dot{m}^2/\rho A^2 \qquad (22)$$

Replacing (22) in (21) yields

$$T\,ds = (C_f/2)\,(\dot{m}^2/\rho^2 A^2)\,C\,dL \qquad (23)$$

Now a similar differential entropy change will be developed from purely thermodynamic considerations for an adiabatic polytropic compression. Referring to Figure 3, the polytropic efficiency is defined to be $\eta_p = \dfrac{dT_{is}}{dT}$ or using the isentropic relations for a differential compression

$$(T + dT_{is})/T = (P + dp/p)^{\frac{\gamma-1}{\gamma}} \qquad (24)$$

Expanding in a binomial series and neglecting higher order terms

$$(1 + dp/p)^{\gamma/\gamma-1} = 1 + \frac{\gamma}{\gamma-1}\,\frac{dp}{p} + \text{higher ORDER TERMS} \qquad (25)$$

Replacing (25) in (24) and rearranging

$$dT_{is}/dT = (T/dT)\,(dp/p)^{\frac{\gamma-1}{\gamma}} \qquad (26)$$

using $\eta_p = dT_{is}/dT$

$$dT/T = (\gamma-1)/(\eta_p \gamma)\, dp/p \tag{27}$$

Introducing the perfect gas law and $c_p = R\frac{\gamma}{\gamma-1}$ into the first law of thermodynamics yields

$$T ds = R(\gamma/\gamma-1)\, dT - (RT/p)\, dp$$

or

$$ds = R\left[(\gamma/\gamma-1)\, dT/T - dp/p\right] \tag{28}$$

The final differential entropy form results by using (27) in (28)

$$ds/R = (1/\eta_p - 1)\, dp/p \tag{29}$$

In order to combine the geometric and thermodynamic developments the differential entropy changes, (29) and (23), can be equated

$$(C_f/2T)\, \frac{\dot{m}^2}{\rho^2 A^3}\, C\, dL = R(1/\eta_p - 1)\, dp/p \tag{30}$$

Introducing the dimensionless referred mass flow rate $\dot{m}_r = \frac{\dot{m}\sqrt{RT_1}}{P_1 A_1}$ into (30) yields

$$(C_f/2T)(\dot{m}_r^2 A_1^2 P_1^2 / RT_1 \rho^2 A^3)\, C\, dL =$$

$$(T/\rho)(1/\eta_p - 1)\, dp/p \tag{31}$$

again using the perfect gas law $\rho = P/RT$

$$(P_1/\rho)(C_f/2T)(\dot{m}_r^2 A_1^2/A^3)\, C\, dL =$$

$$(T/\rho)(1/\eta_p - 1)\, dp \tag{32}$$

rearranging

$$(C_f/2)\,(\dot m_r^2\,A_1^2/A^3)\,C\,dL = (P/\rho_1)(1/\eta_p - 1)\,d(P/P_1) \quad (33)$$

For a polytropic process $P/\rho^n$ = constant so (33) becomes

$$(C_f/2)\,\dot m_r^2\,(A_1^2/A^3)\,C\,dL = (1/\eta_p - 1)(P/P_1)^{1/n}\,d(P/P_1) \quad (34)$$

The equation is now in a suitable form to be integrated. Vavra has called the left side $dX_1$ and integrated it from the channel entrance to exit along s streamline so that the constant total enthalpy assumption is valid.

$$\int_0^L dX_1 = \int_0^L (C_f/2)\,\dot m_r^2\,(A_1^2/A^2)\,C\,dL \quad (35)$$

As previously discussed $C_f$ is a constant representing shear losses and may be brought outside the integral. Also referred flow is a constant for a given flow rate.

$$\int_0^L dX_1 = (C_f/2)\,\dot m_r^2 \int_0^L (A_1^2/A^3)\,C\,dL \quad (36)$$

The integral of (36) contains geometric characteristics of the diffuser and has been defined as the shape parameter omega ($\Omega$).

$$\Omega \equiv \int_0^L (A_1/A)^3\,(C/A_1)\,dL \quad (37)$$

The product $\Omega\,C_f$ must be related to diffuser performance for $\Omega$ to be useful. In order to do this the right side of (34) must also be integrated.

$$dX_2 = (1/\eta_p - 1)\,(P/P_1)^{1/n}\,d(P/P_1)$$

Integrating as before from entrance to exit.

$$X_2 = \int_1^{P_2/P_1} (1/\eta_p - 1)\,(P/P_1)^{1/n}\,d(P/P_1) \quad (38)$$

By assuming constant polytropic efficiency and n constant

$$X_2 = (1/\eta_p - 1)(n/n+1)\left((P_2/P_1)^{1+1/n} - 1\right) \quad (39)$$

For the differential change $P_2 = P_1 + \Delta P$ with $\Delta P << P_1$ and again using a binomial expansion

$$[(P_1 + \Delta P)/P_1]^{\frac{n+1}{n}} = 1 + (n+1/n)\,\Delta P/P_1 \quad \text{+ higher order terms}$$

replacing in (39)

$$X_2 = (1/\eta_p - 1)\,\Delta P/P_1 \quad (40)$$

equating (36) and (40)

$$(C_f/2)\,\dot{m}_r^2 \int_0^L (A_1/A)^3 (C/A_1)\, dL =$$

$$(C_f/2)\,\dot{m}_r^2\,\Omega = (1/\eta_p - 1)\,\Delta P/P_1 \quad (41)$$

substituting for $\dot{m}_r$ according to the definition

$$\dot{m}_r = \rho_1 A_1 V_1 \sqrt{RT_1} / P_1 A_1$$

gives

$$(C_f/2)(\rho_1^2 A_1^2 V_1^2 RT_1)\,\Omega/(P_1^2 A_1^2) = (1/\eta_p - 1)\,\Delta P/P_1$$

or

$$\Omega\, C_f = (2\Delta P/\rho_1 V_1^2)(1/\eta_p - 1) \quad (42)$$

Since constant total enthalpy was assumed there is no change in total temperature so rewriting (28)

$$dS = -R\,(dP_t/P_t) \quad (28a)$$

equating (29) and (28a)

$$-dP_t/P_t = (1/\eta_p - 1)\,dP/P \quad (29a)$$

(29a) is in a suitable form to be integrated and is a straightforward log.

$$(-\ln P_t)_1^{P_{t_2}/P_{t_1}} = (1/\eta_p - 1)\,[\ln P]_1^{P_2/P_1}$$

or

$$\ln(P_{t_1}/P_{t_2}) = (1/\eta_p - 1)\ln(P_2/P_1) \qquad (43)$$

again using

$$P_{t_1}/P_{t_2} = P_{t_1}/(P_{t_1} + \Delta P_t) \quad \text{and} \quad P_2/P_1 = 1 + \Delta P/P_1$$

with the usual expansion for logs; i.e. ln(1+x) = x, (43) becomes

$$\Delta P/P_1\,(1/\eta_p - 1) = -\Delta P_t/P_{t_1} \qquad (44)$$

or

$$(1/\eta_p - 1)\,\Delta p = -\Delta P_t\,(P_1/P_{t_1}) = -\Delta P_t/(1 + \tfrac{\gamma}{2} M_1^2) \qquad (45)$$

All flow considered was incompressible with $M_1 \ll 1$ so

$$(1/\eta_p - 1)\,\Delta p = -\Delta P_t \qquad (46)$$

replacing (46) in (42)

$$\Omega C_f = -2\,\Delta P_t\,(\rho_1 V_1^2) = (P_{t_1} - P_{t_2})/(\tfrac{1}{2}\rho_1 V_1^2) \qquad (47)$$

or

$$(P_{t_1} - P_{t_2})/(\tfrac{1}{2}\rho V_1^2) = (P_1 + \tfrac{1}{2}\rho V_1^2 - P_2 - \tfrac{1}{2}\rho V_2^2)/(\tfrac{1}{2}\rho V_1^2) =$$

$$\Omega C_f \qquad (48)$$

However $C_p$ = coefficient of pressure

$$C_p = (P_2 - P_1)/(\tfrac{1}{2}\rho V_1^2) \tag{49}$$

$C_{p_i}$ = pressure recovery if the process followed the $P_1$ to $P_{2_{isen}}$ line of Figure 3, i.e. ideal.

$$C_{p_i} = (P_{2_{isen}} - P_1)/(\tfrac{1}{2}\rho V_1^2) \tag{50}$$

For isentropic flow $\Delta P_t = 0$ so (50) becomes

$$C_{p_i} = (\rho/2 V_1^2 - \rho/2 V_2^2)/(\tfrac{1}{2}\rho V_1^2) = 1 - (A_1/A_2)^2 \tag{50a}$$

Replacing (50a) in (37) gives

$$(P_{t_1} - P_{t_2})/(\tfrac{1}{2}\rho V_1^2) =$$

$$[P_1 + \tfrac{1}{2}\rho V_1^2 - P_2 - \tfrac{1}{2}\rho V_1^2(1 - C_{p_i})]/(\tfrac{1}{2}\rho V_1^2) \tag{51}$$

using (49) and (48) in (51) yields

$$\Omega C_f = C_{p_i} - C_p \tag{52}$$

(52) is the basic result of the theory. The amount a flow departs from isentropic conditions has been shown to be a product of the geometric parameter omega and an average shear stress coefficient.

DIFFERENTIAL FLUID ELEMENT

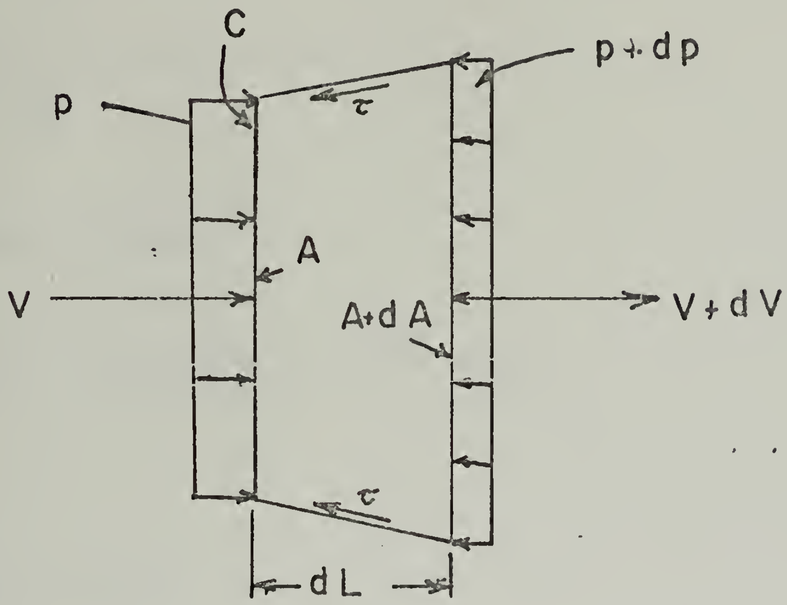

dL = DIFFERENTIAL LENGTH
A = FLOW AREA
p = STATIC PRESSURE
τ = SHEAR
V = VELOCITY
C = WETTED PERIMETER

FIGURE 2

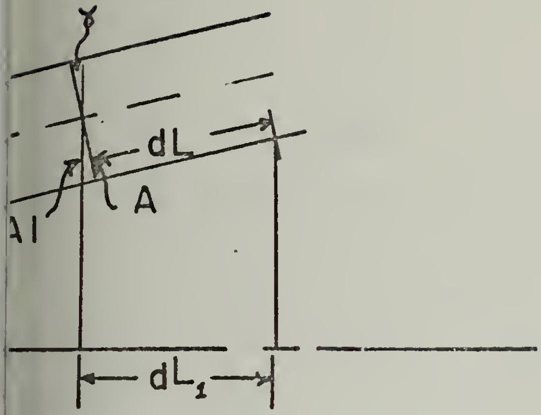

FIGURE 2 (a)

ANNULAR CHANNEL SECTIONS

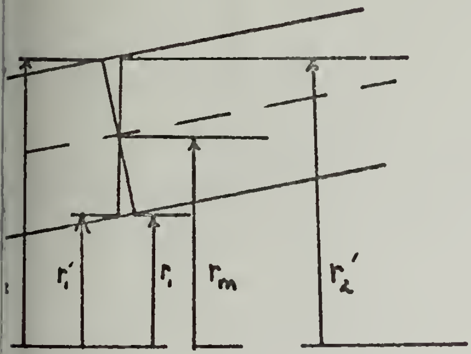

FIGURE 2 (b)

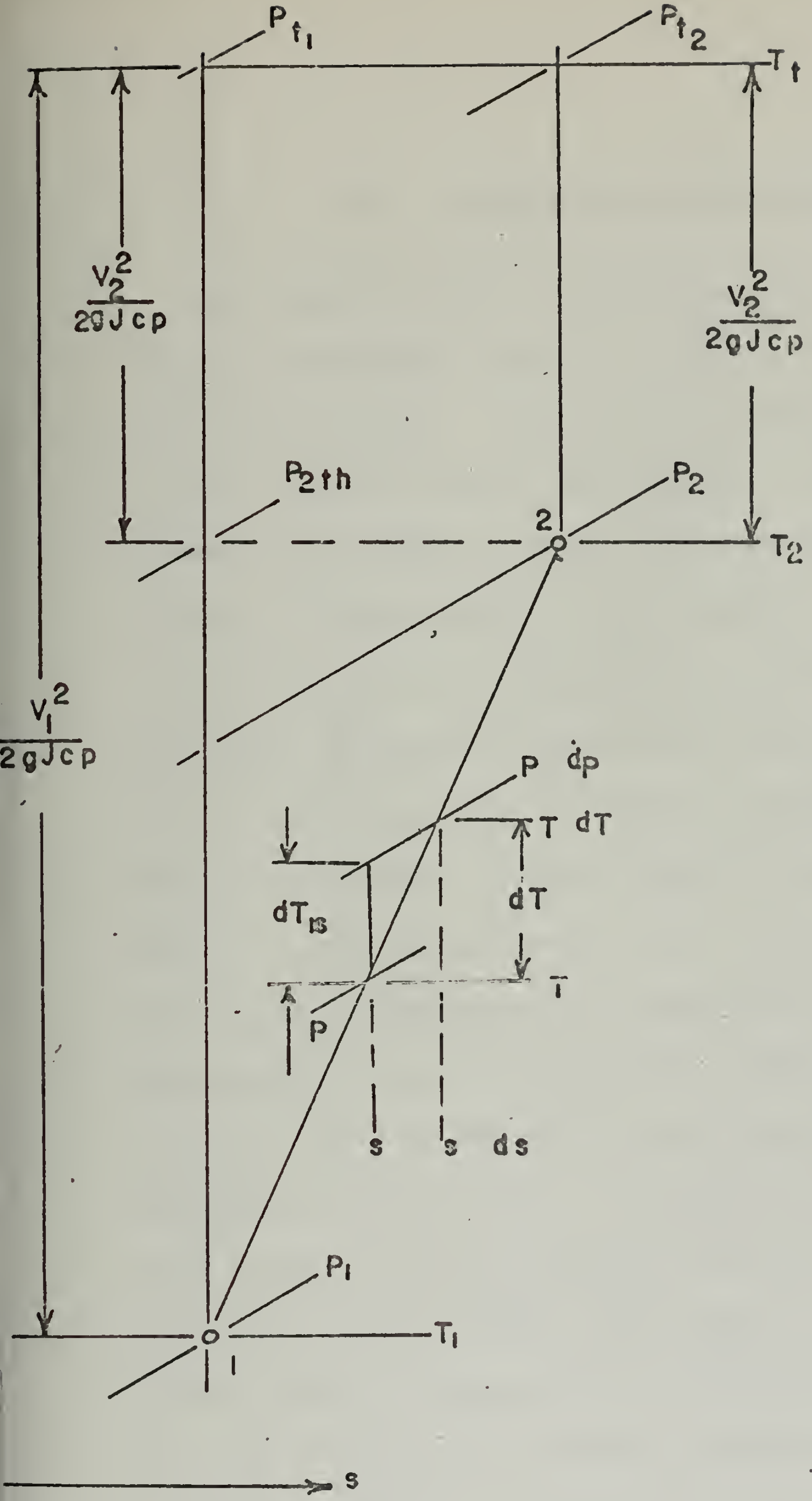

FIGURE 3

T-s diagram for an adiabatic compression

## III. ORIGINAL SUGGESTION FOR USE OF OMEGA

Once equation (52) was derived, Vavra [Ref. 8] investigated some two dimensional data by plotting the losses as a function of the shape parameter. His plot is reproduced in Figure 4. It can be seen that the losses tend towards a minimum value in the neighborhood of an omega of ten. For this reason Vavra suggested that an omega of ten might be a good diffuser design value.

In an earlier investigation of the shape parameter, Gapp [Ref. 3] reduced the annular data of Sovran and Klomp [Ref. 6] so that a plot similar to Figure 4 could be generated as shown in Figure 5. Although the plot shows the same trends as Vavra's graph, there does not seem to be a value of omega to insure minimum losses. Additional two dimensional data of Kline [Ref. 5] was also plotted and has very similar characteristics, but does not offer any firm evidence that one value of omega is to be strongly preferred over any other. A somewhat different approach was to plot lines of constant omega on the two dimensional flow regime chart Fox and Kline [Ref. 5], Figure 6. It was seen, however, that a given value of omega did not necessarily indicate the state of the flow. Although the above evidence indicates that Vavra's original suggestion of how best to represent losses as a function of omega was not the best implementation of the shape parameter, it does not adversely reflect on the validity of omega as a good parameter. Omega has a definite physical significance which is fundamentally different from previously suggested parameters embodying all pertinent geometric characteristics. A derivation

of the physical meaning of omega has already been given and an additional aspect of omega will be given in a later section.

The effort to achieve small losses as reflected in a minimum value of $\Omega C_f$ may not always be the chief goal of a particular diffuser. The ideal pressure recovery coefficient is a function of area ratio and as such is a measure of the maximum diffusion obtainable for a particulr geometry. If the designer wishes a diffuser to convert a large portion of the flow evergy into pressure, a larger area ratio is called for. However if only a modest rise is called for with a fairly uniform exit profile the reverse is true. The application calling for a large pressure rise may be able to tolerate higher losses when maximizing recovery while the need for a uniform velocity profile will tend to require minimum losses In proposing a theory or correlation for performance the two above conditions must be considered so that an optimum design criterion may be formulated. Before investigating diffuser characteristics further a somewhat simpler derivation of omega will be given to relate the shape parameter to diffuser performance in a different way than previously derived.

VAVRA'S PLOT OF SOME 2-D DATA

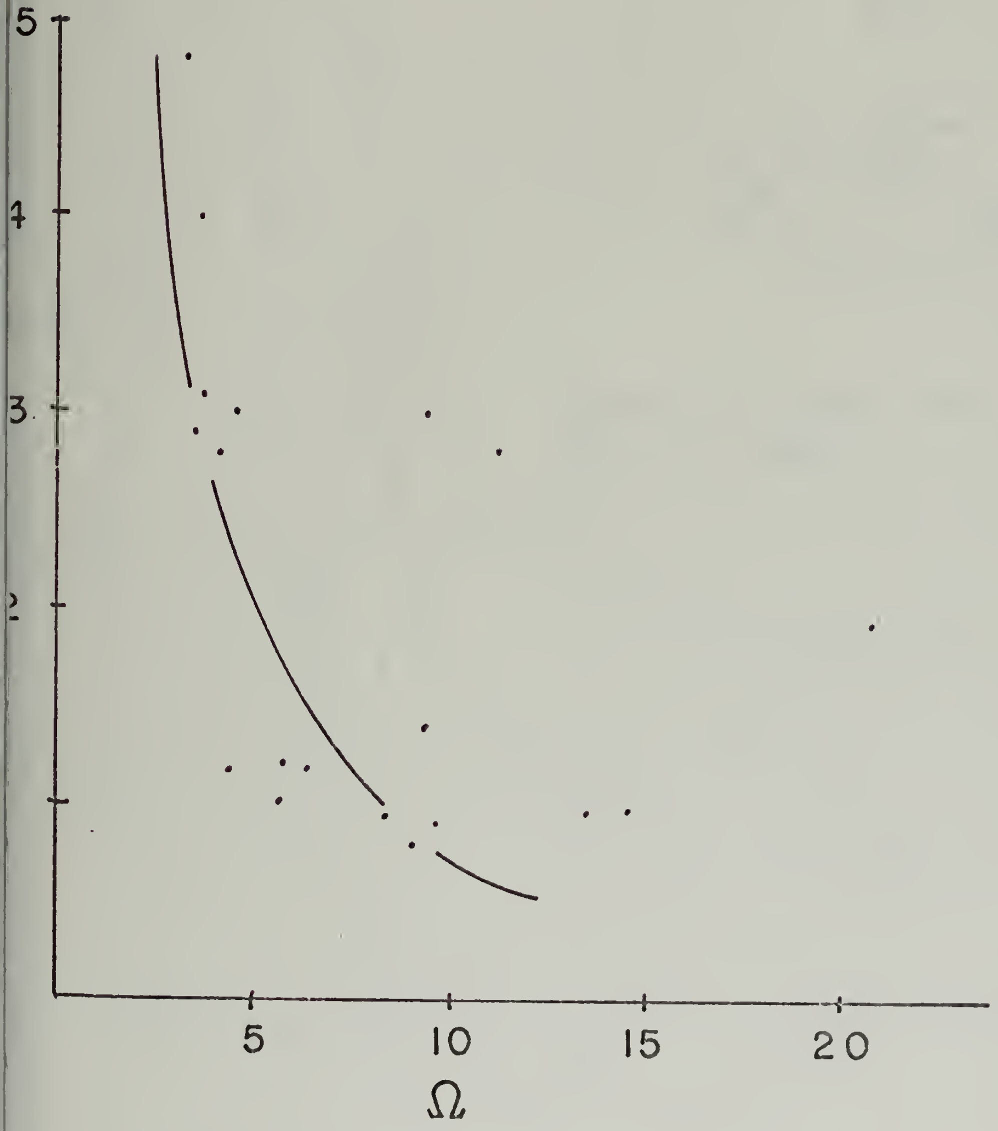

FIGURE 4

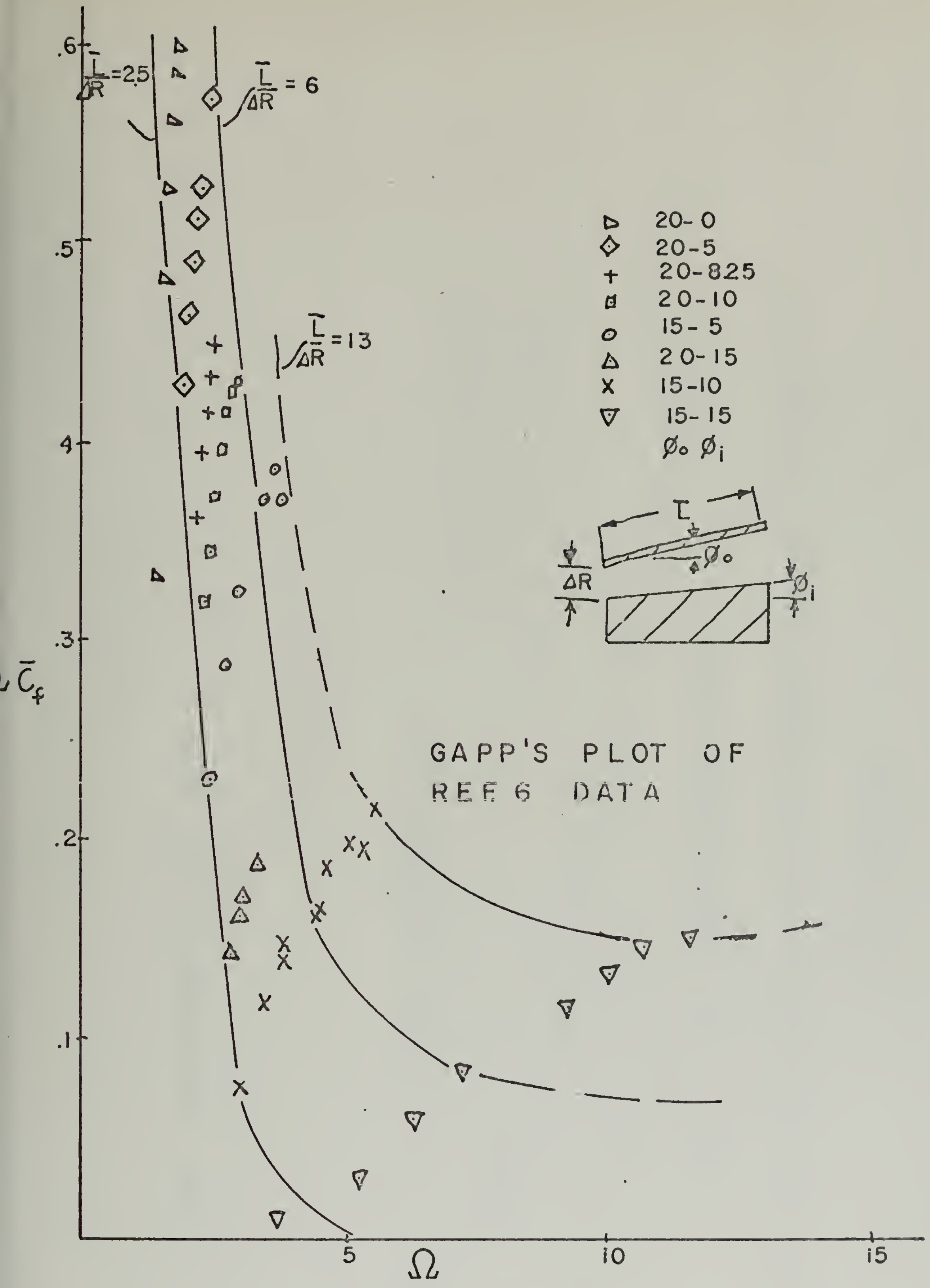

.6
.5
.4
.3
.2
.1
$\bar{C}_f$
5
10
15
$\Omega$
$\frac{L}{\Delta R}=2.5$
$\frac{L}{\Delta R}=6$
$\frac{L}{\Delta R}=13$
▷ 20-0
◇ 20-5
+ 20-825
□ 20-10
○ 15-5
△ 20-15
x 15-10
▽ 15-15
$\phi_o$ $\phi_i$
L
$\Delta R$
$\phi_o$
$\phi_i$
GAPP'S PLOT OF REF 6 DATA

FIGURE 5

2-D FLOW REGIMES OF REF 5

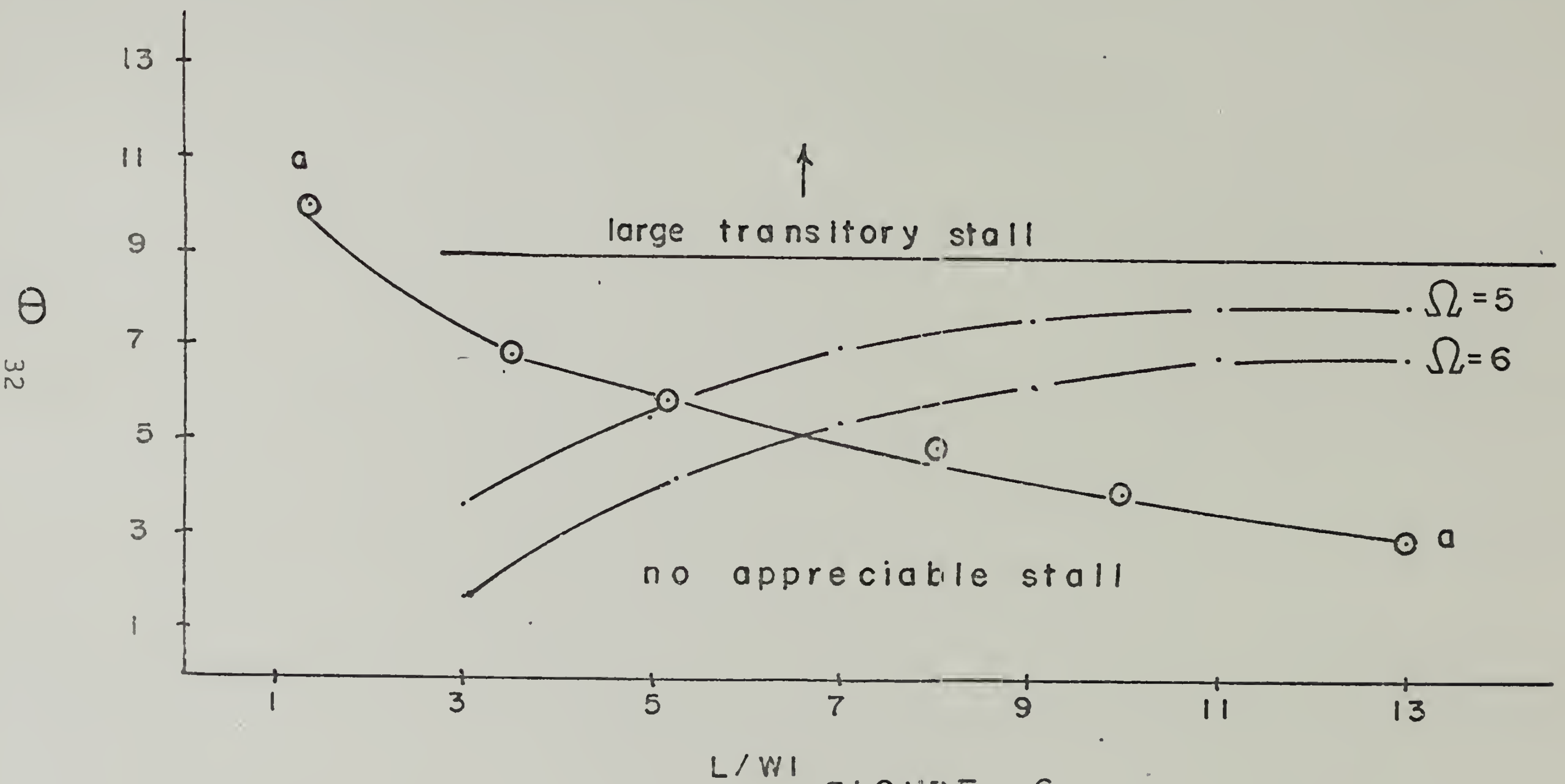

FIGURE 6

## IV. AN ALTERNATE DERIVATION OF OMEGA

The non dimensional group used to define omega was a logical consequence of the combination of the momentum theorem for an arbitrary channel and the expression for a differential entropy rise in an adiabatic polytropic compression. The derivation was necessarily lengthy and the expression for omega may be obtained from a more basic approach.

For the same one dimensional channel flow of Figure 2

$$P_t = p + \tfrac{1}{2}\rho V_1^2 \tag{53}$$

$$\dot{m} = \rho A V = \rho_1 A_1 V_1 \tag{54}$$

Taking the derivative of (53) with respect to length and assuming constant total pressure

$$dP_t = dp + \rho V dV = 0 \tag{55}$$

and from continuity for constant density

$$V\,dA = -A\,dV$$

or

$$V\,dV = (-V^2/A)\,dA \tag{56}$$

replacing (56) in (55) gives

$$\rho V^2\,dA/A = dp \tag{57}$$

and using the definition of mass flow from (54)

$$dp = (\rho \dot{m} / \rho^2 A^3)\,dA = \rho V_1^2 (A_1^2/A^3)\frac{dA}{dL}\,dL \tag{58}$$

rearranging

$$dp/(\tfrac{1}{2}\rho V_1^2) = 2\,(A_1/A)^3\,(1/A_1)\,(dA/dL)\,dL \qquad (59)$$

and integrating both sides

$$C_{p_i} = 2\int_0^L (A_1/A)^3\,(1/A_1)\,(dA/dL)\,dL \qquad (60)$$

The integral in (60) looks very much like the definition of omega, but the area rate of change must be related to the wetted perimeter for each diffuser type.

A. CONICAL

$$A(L) = 2\pi\,(R_1 + L\,TAN\,\theta)^2 \qquad (61)$$

$$dA/dL = 2\pi\,TAN\,\theta\,(R_1 + L\,TAN\,\theta) \qquad (62)$$

$$C(L) = 2\pi\,(R_1 + L\,TAN\,\theta) \qquad (63)$$

combining (63) and (62) yields

$$C(L) = (dA/dL)/TAN\,\theta \qquad (64)$$

and replacing (64) in (60)

$$C_{p_i} = 2\int_0^L (A_1^2/A^3)\;C(L)\;TAN\,\theta\;dL = 2\,TAN\,\theta\,\Omega \qquad (65)$$

Therefore for the conical case the ideal pressure rise is a function of the wall angle and omega. The factor relating $C_{p_i}$ to omega has been defined as PAR4C.

## B. TWO DIMENSIONAL

$$dA/dL = 2B_1 \, TAN\theta \tag{66}$$

$$C(L) = 2B_1 + 2W_1 + 4\,LTAN\theta = 2B_1 + 2W(L)$$

or

$$2B_1 = C(L) - 2W(L) \tag{67}$$

combining (66) and (67)

$$dA/dL = C(L)\,TAN\theta\,(1 - 2W(L)/C(L)) \tag{68}$$

$$C_{P_i} = \int_0^L 2TAN\theta\,(1 - 2W(L)/C(L))\left(\frac{A_1}{A}\right)^3\left(\frac{C(L)}{A_1}\right)dL \tag{69}$$

Equation (69) is also similar to the expression for omega, but an investigation has shown that $C_{P_i}$ is not related to omega by a simple constant analogous to that of the conical diffuser.

## C. ANNULAR

An annulus is a complicated shape, but it shares certain fundamental geometric characteristics of the cone such as axial symmetry. In fact, an annular diffuser is nothing more than a conical diffuser with an axisymmetric center body. For an annular diffuser:

$$\begin{aligned} dA/dL = {} & 2\pi L\,(TAN^2\theta_0 - TAN^2\theta_i) \\ & + 2\pi\,(RT1\;TAN\theta_0 - RH1\;TAN\theta_i) \end{aligned} \tag{70}$$

$$C(L) = 2\pi\,[\,R_0(L) + R_I(L)\,] \tag{71}$$

$$dA/dL = \left[\frac{(TAN\,\theta_o\,R_o(L) - TAN\,\theta_i\,R_I(L))}{(R_I(L) + R_o(L))}\right] C(L) \qquad (72)$$

By examining the factor relating area gradient to the local circumference in (72), it can be seen that an expression similar to (65) can be derived for annular diffusers. The factor is defined as PAR4A.

$$PAR4A \equiv [TAN\,\theta_o\,R_o(L) - TAN\,\theta_i\,R_I(L)]/[R_I(L) + R_o(L)]$$

By referring to Figure 7 and making use of the theorum relating similar triangles from geometry it can be seen that PAR4A may also be expressed as a function of the inlet geometry.

$$PAR4A = \frac{TAN\,\theta_o\,(RT1/L_{in})\,L - TAN\,\theta_i\,(RH1/L_{in})\,L}{(RH1/L_{in})\,L + (RT1/L_{in})\,L}$$

$$= (TAN\,\theta_o - RRAT\;TAN\,\theta_i)/(1 + RRAT)$$

RRAT = inlet radius ratio = $RH1/RT1$

It can be seen that PAR4A is constant for a given annular diffuser family. A family is defined as a set of diffusers with constant inner and outer wall angles and the same radius ratio. For example all diffusers with wall angles of 15 and 20 degrees with a radius ratio of one half would comprise one family while all diffusers with wall angles of 10 and 25 degrees with a radius ratio of .7 would comprise another family. The previous derivation may be used in (52)

$$\Omega\,C_f = C_{p_i} - C_p \qquad (52)$$

or

$$\omega C_f = C_{p_i} (1 - C_p / C_{p_i})$$

$$C_f = (C_{p_i}/\omega) (1 - C_p / C_{p_i}) =$$
$$\mathrm{PAR4} \ (1 - C_p / C_{p_i}) \tag{52a}$$

Although the previous derivation of omega does not allow direct calculation of performance, it does give a better understanding of the shape parameter. Once the above derivations were formulated a parameter study was undertaken to observe the response of omega to certain geometric factors for each diffuser shape.

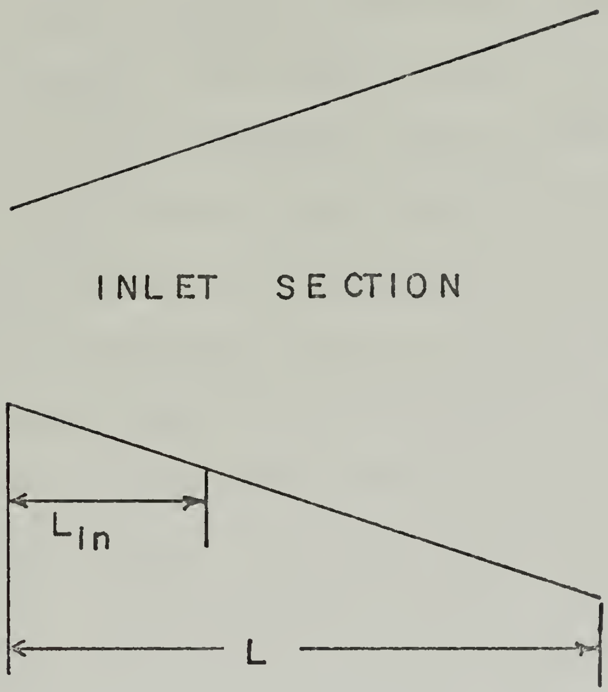

FIGURE 7

# V. PARAMETER STUDY

The parameter study was done with the aid of several computer programs which are listed and explained in Appendix A. To do a complete study would have been a major undertaking with all the associated variables of conical, two dimensional, and annular diffusers. However, a representative study was done by varying each parameter a reasonable number of times to establish trends. The conical diffuser was the simplest shape and was studied first.

The conical variables were taken as inlet area, length, and wall angle; but to have a manageable amount of data the inlet area was set equal to unity and the other parameters were varied. Figure 8 shows that omega is a strong function of wall angle and past a certain non dimensional length, the wall angle dominates. For a high divergence angle the characteristic length is short before a constant omega is achieved while the opposite is true for the lower divergence angles. The wall angle is inversely proportional to the final value of omega as shown in Figure 8. An interesting fact about Figure 8 is that an omega of ten results for a wall angle of about three degrees. Conical diffusers with small divergence angles have low losses, but they do not necessarily have the highest pressure recovery for lengths common in practice. A better look at omega in relation to flow conditions was found by plotting constant omega lines on the two dimensional flow regime chart of Fox and Kline [Ref. 5].

Figure 6 was briefly mentioned earlier, but there are several aspects of the plot that were not discussed. For the two

dimensional geometry, omega was found to be dependent on angle, length, and inlet geometry. As Figure 6 demonstrates, a particular value of omega in the two dimensional regime can indicate a full range of flow conditions from unstalled to large transitory stall. In addition to not indicating conditions in the two dimensional diffuser, the constant omega line takes on different values depending upon the inlet geometry.

Finally the characteristics of annular diffusers were studied. The annular diffuser is the shape of most interest for turbomachinery applications and unfortunately is the least understood. There are numerous parameters to vary: wall length, radius difference, mean radius, inner wall angle, and outer wall angle. Due to the large number of variables no plots analogous to Figure 6 and Figure 7 were apparent to show omega trends. However, one graph which combined inlet geometry and wall angles was plotted versus non dimensional length. Figure 9 has the advantage of incorporating as many geometric parameters as possible into a meaningful group by plotting area rate of change versus length at a constant value of omega. The area rate of change is about constant for a given set of wall angles and inlet geometry as can be seen from (70) when $(TAN^2\theta_o - TAN^2\theta_i)$ can be neglected, and it is also related to the pressure gradient. The plot shows the same general trends as the other two geometries by indicating the omega dependence on area rate of change and length. The figures all show that high omegas can only be achieved with low area rate of change, but several geometric conditions may result in low values. A diffuser may be very short or have a high area

gradient in the case of a low omega value. Although the parameter study indicated geometric trends, it did not offer any insights into performance. To gain an understanding of diffuser performance the published data was analyzed more closely.

CONSTANT Ω LINES FOR A CONICAL DIFFUSER

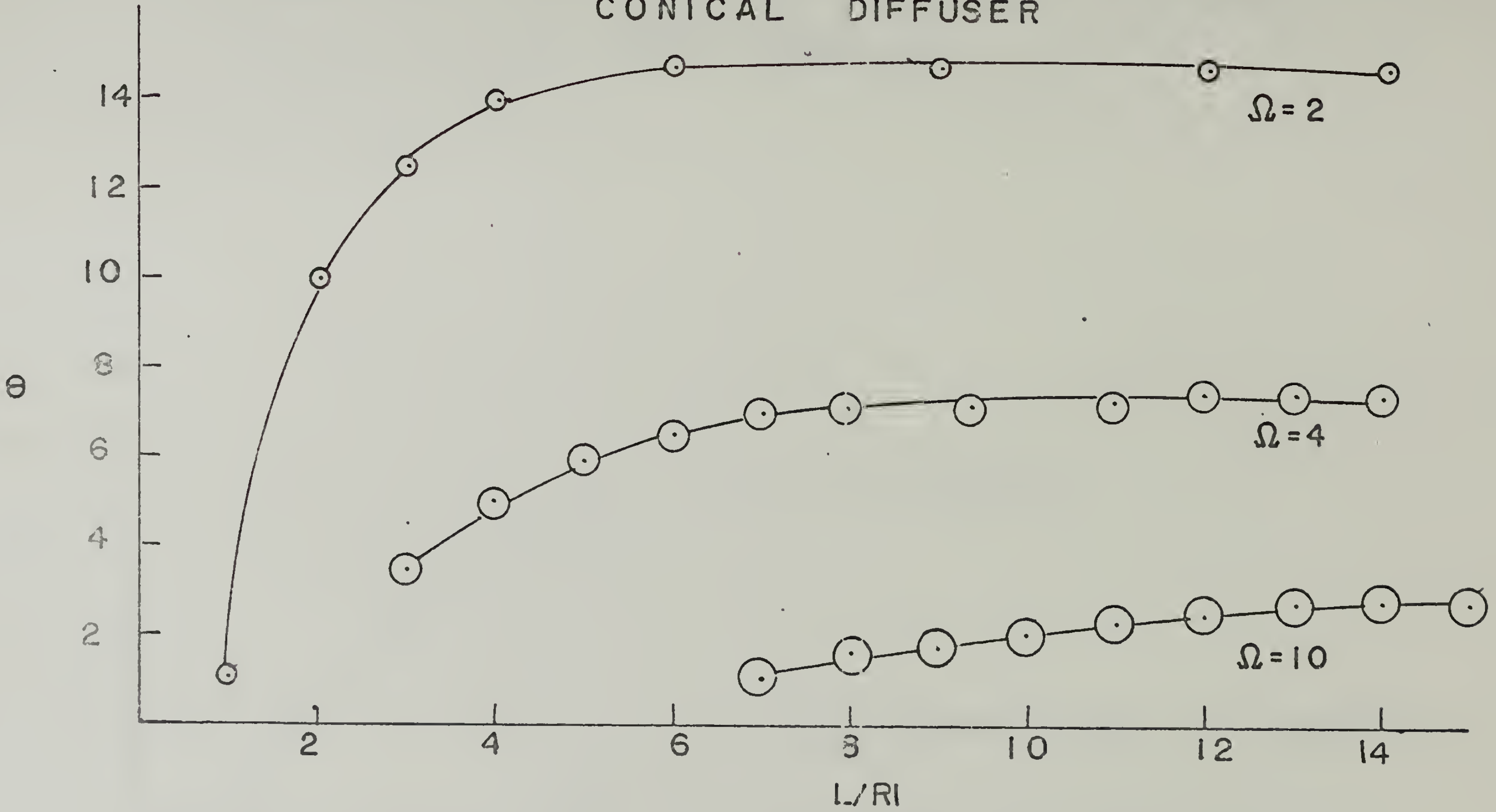

FIGURE 8

## CONSTANT $\Omega$ LINES FOR ANNULAR DIFFUSERS WITH A GIVEN INLET GEOMETRY

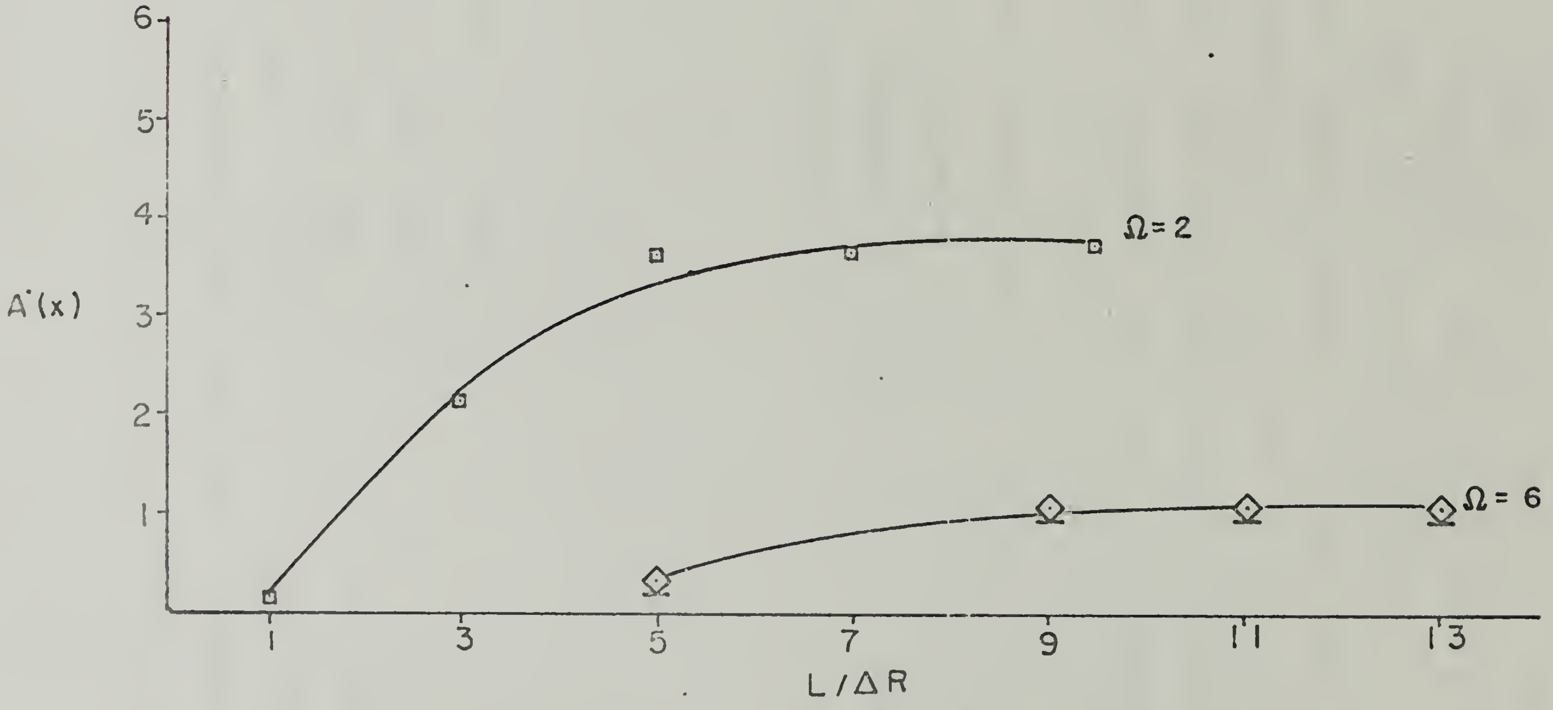

FIGURE 9

## VI. DATA CORRELATIONS

Previous attempts to predict or explain diffuser performance relied on a number of parameters and graphs that were rather unweildy to use, or an oversimplified approach such as the equivalent cone angle method was employed. Gapp [Ref. 3] looked at the data of Sovran and Klomp [Ref. 6] in the manner suggested by Vavra [Ref. 8] and tested several diffusers, but he was unable to develop a method of prediction based on his work. It has been shown in previous sections that the parameter omega has physical significance in relation to diffusing flows, and it was reasonable to assume that omega is in some way related to performance. If some means of determining the shear term, $C_f$, could be found; equation (52) would give performance directly. Several attempts were made to arrive at a technique for determining $C_f$, but some other methods of predicting performance from curves bear mentioning first.

If $\Omega C_f$ is small the recovery is very close to ideal, but $\Omega C_f$ must be minimized for a given area ratio to insure maximum pressure recovery. This fact suggested a possible utilization of the original plot of Vavra. By drawing lines of constant area ratio on an $\Omega$ versus $\Omega C_f$ graph, an optimum omega range can be determined at the given area ratio. For the given area ratio, the omega range would guarantee minimum losses and maximum pressure recovery close to the desired one. A plot such as Figure 10, which is a line of area ratio two from the data of Sovran and

Klomp [Ref. 6], would result. It shows an omega range of five to eight for minimum losses. Unfortunately Sovran and Klomp did not have a wide range of area ratios, and to do the required testing to generate other data would be very costly and time consuming.

Another plot was discovered, but it did not have a wide range of applicability. However, it is worth mentioning since it correlated a large amount of the annular data of Sovran and Klomp. The non dimensional area gradient, $(dA/dL)/AR$, is related to the pressure gradient, as shown in (57). After several attempts to relate the area gradient to losses a graph such as Figure 11 was plotted. It is a plot of non dimensional area gradient versus losses for a given non dimensional length, and a straight line resulted for a range of lengths. The resultant straight lines suggested plots such as Figures 12 and 13 in an attempt to correlate all the annular data. Figure 12(a) is a list of symbols used in Figures 12 - 15. However, considerable scatter is evident in addition to some definite trends. Two distinct lines are visible and some data considerably off both curves. The two distinct lines correspond to families with inlet radius ratios of .55 and .70 respectively. The data below the lines are from families with inner and outer wall angles that differ by no more than two degrees. These plots are of limited value at best and are rendered even more questionable because the diffusers with the best recovery, the families with similar inner and outer wall angles, do not even fall on the curves.

The independent derivation of omega introduced a geometric parameter that related the ideal recovery to omega (see equations (52) through (72). The parameter, PAR4, had a different form for each class of diffuser, but in all cases it corresponded to the quotient of the area gradient and circumference for a given axial station. If the shear stress coefficient could be determined, the theory of Vavra would give performance directly from equation (52). To see if the parameter, which has been designated PAR4A and PAR4C, had any relation to the shear stress coefficient, Figure 14 was plotted with the conical data of Cockrell and Markland [Ref. 2] and annualar data from Sovran and Klomp. The conical data consisted of twenty-four diffusers which were tested at two boundary layer thicknesses and approximately eighty annular diffusers. No information was given concerning the exact dimensions of the inlet boundary layer for the annular tests, but all the annular diffusers were tested on the same apparatus with a thin inlet boundary layer. The set of conical diffusers which is displaced upwards on the curve had a thicker inlet boundary layer and exhibited the expected higher losses. Some scatter is evident in the figure for the longer annular diffusers, but a definite curve is discernable.

Once Figure 14 was established, the next logical step was Figure 15. To enable the direct determination of recovery from a known omega, PAR4 was plotted versus the quotient of pressure recovery and omega. Again a good curve with small scatter resulted. The conical data with the thick inlet boundary layers were displaced downwards as expected. Figure 15 differs from the previous

annular correlation in that the data fall close to the line, and the wide scatter attributed to families with similar inner and outer wall angles is not present. Also the curve does not seem to depend on inlet radius ratio. With Figure 15 and a knowledge of geometry for a conical or annular diffuser with a thin inlet boundary layer thickness, the pressure recovery can be determined.

Besides predicting the recovery, the correlation presented in Figure 14 can be utilized in the development of optimization criteria. The designer is often faced with the problem of maximizing the recovery for a given length. The annular case will be discussed, but the development for a conical diffuser is similar. It was shown that

$$\Omega C_f = C_{p_i} - C_p \qquad \text{and} \qquad C_{p_i} = PAR4\ \Omega$$

Combining the equations gives

$$C_p = C_{p_i}\,(1 - C_f\,/PAR4) \tag{73}$$

However, Figure 14 shows that $C_f$ is a function of PAR4. The curve is of the form $C_f = \alpha\,(PAR4)^b$, where $\alpha$ and $b$ are constants that can be determined from polynomial curve fitting techniques used in numerical analysis. Also the ideal recovery coefficient can be shown to be a function of inlet conditions and non dimensional length.

$$C_{p_i} = 1 - (A_1/A_2)^2$$

$$A_1/A_2 = (RTI + RHI)/\big[RTI + RHI + \Delta R\,(L/\Delta R)^2\,(TAN^2\theta_o - TAN^2\theta_i) + L/\Delta R\,(RTI\,TAN\,\theta_o - RHI\,TAN\,\theta_i)\big] \tag{74}$$

By replacing (74) in the expression for the ideal recovery coefficient and combining this result with an expression for $C_f$ as suggested, the pressure coefficient will be expressed as a function of inlet geometry and non dimensional length. When an expression has been developed, the theory of maxima and minima of a function may be used. By taking the derivative of $C_p$ with respect to non dimensional length and setting the resultant expression equal to zero, the recovery could be maximized. To obtain a given recovery in a minimum length, the correlation could be employed in a similar fashion.

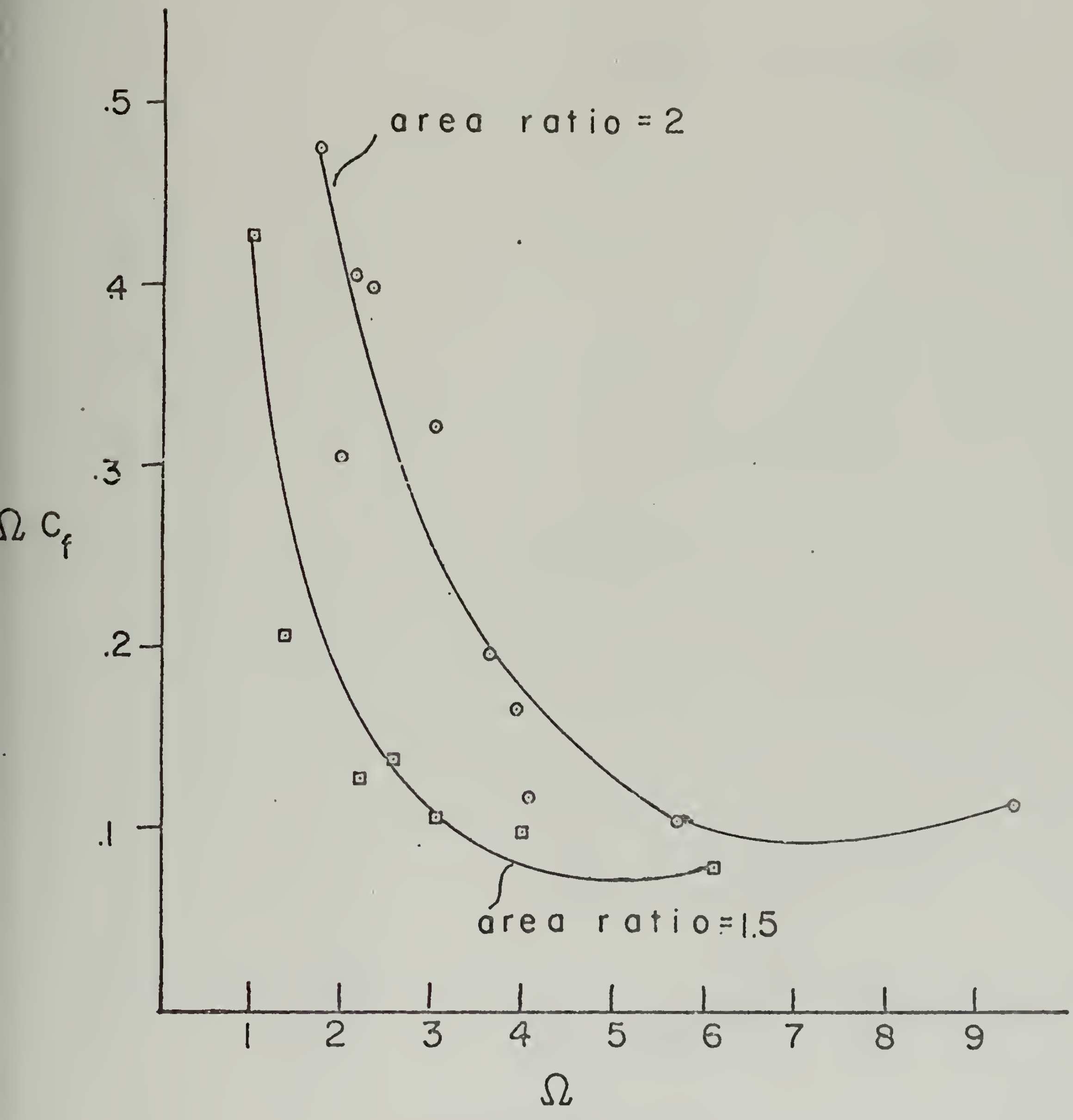

FIGURE 10

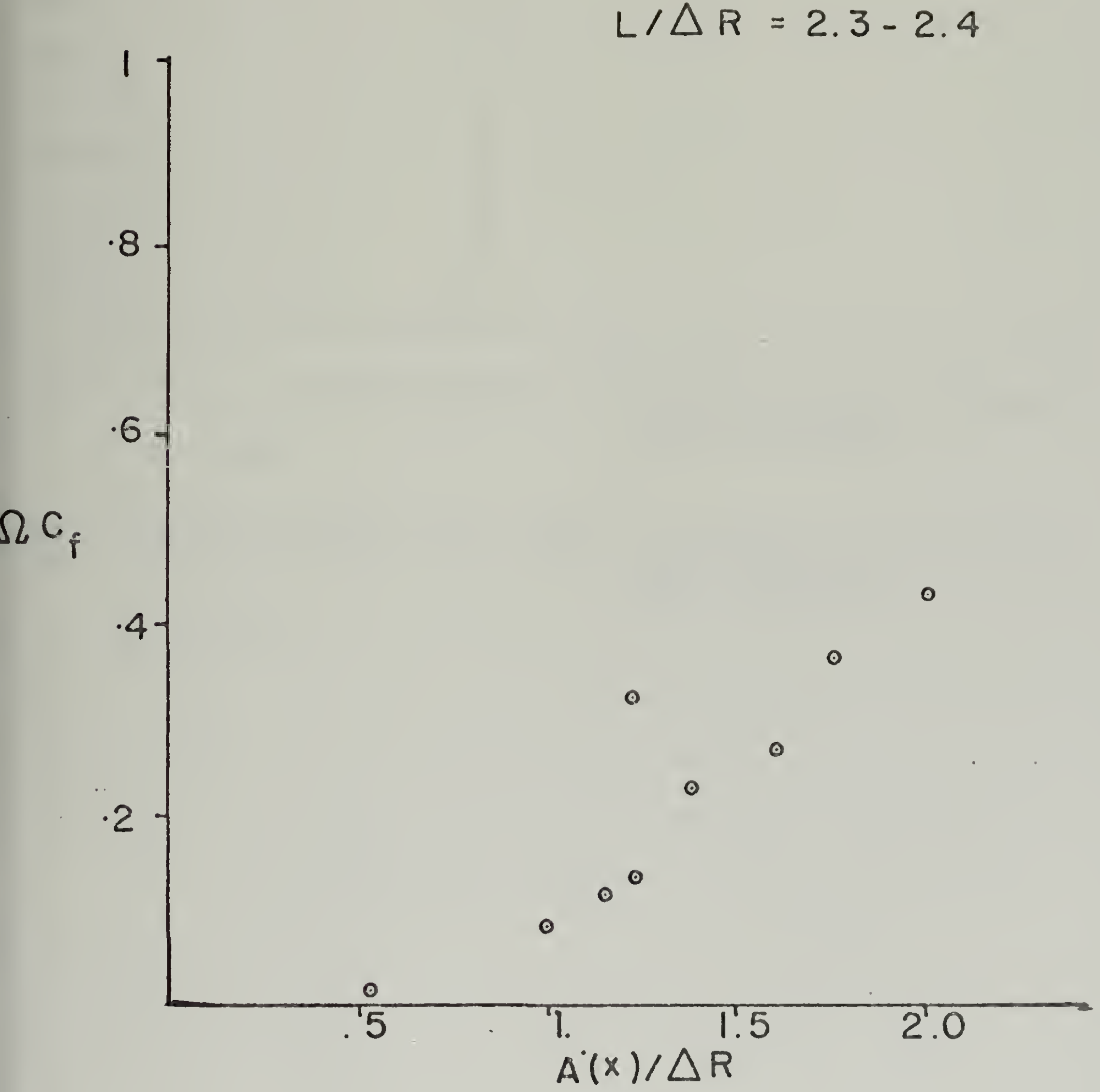

FIGURE II

| FAMILY | SYMBOL |
|---|---|
| 15-15 | · |
| 15-10 | ○ |
| 15- 8 | △ |
| 15-5 | ◬ |
| 20-15 | □ |
| 20- 10 | ⊙ |
| 20- 8 | ◺ |
| 20-5 | ⌂ |
| 30-29 | ⊹ |
| 15- 0 | ⟐ |
| 15-13 | ⏏ |
| 20- 0 | ▭ |

---

⌖ = ref. 2 conical data with $\frac{\text{inlet momentum thickness}}{\text{inlet diameter}}$ of .005

◎ = ref. 2 conical data with $\frac{\text{inlet momentum thickness}}{\text{inlet diameter}}$ of .025

FIGURE 12 (a)

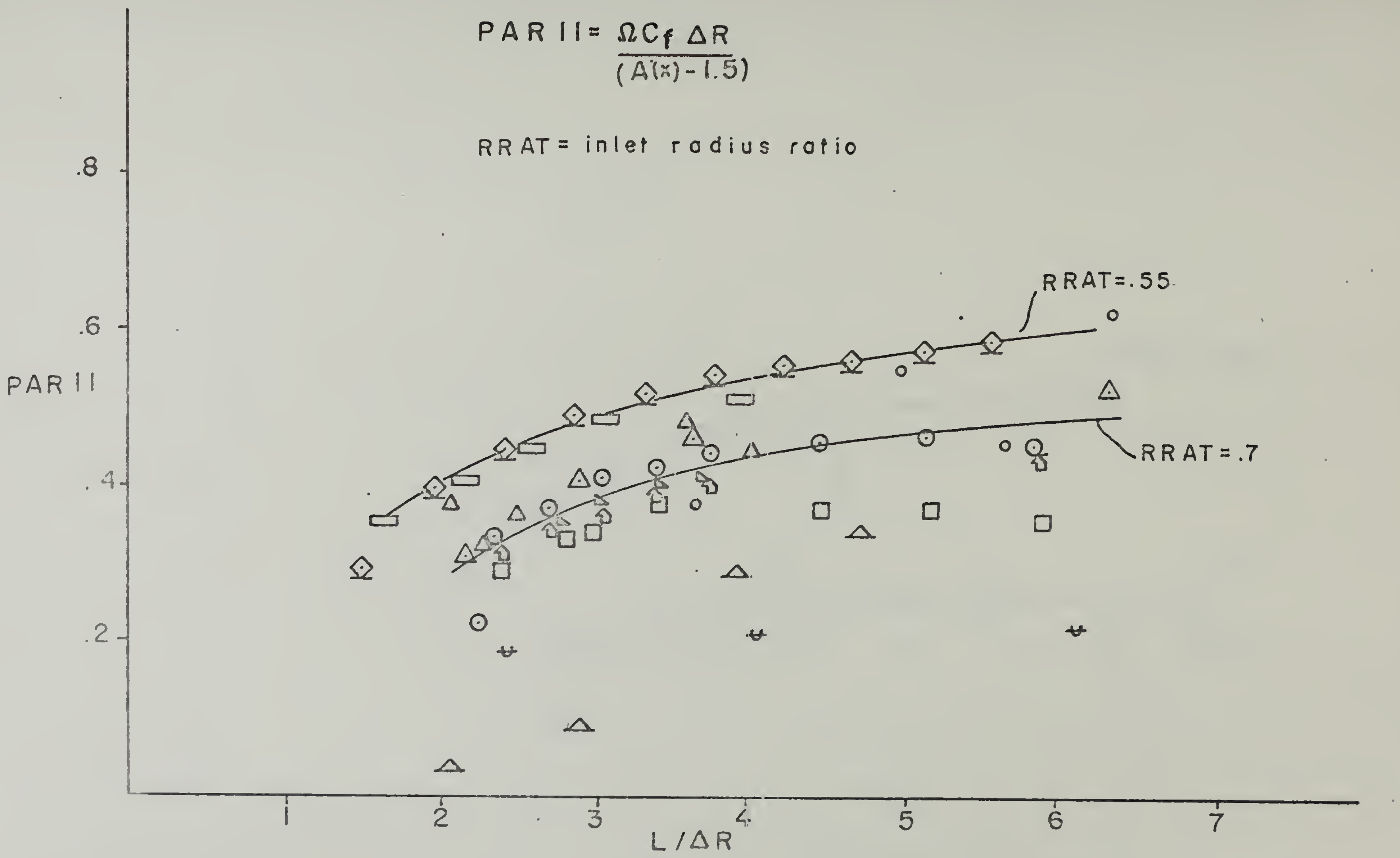
PAR II = $\frac{\Omega C_f \Delta R}{(A(x)-1.5)}$
RRAT = inlet radius ratio
RRAT = .55
RRAT = .7
PAR II
.8
.6
.4
.2
1
2
3
4
5
6
7
L/ΔR

FIGURE 12

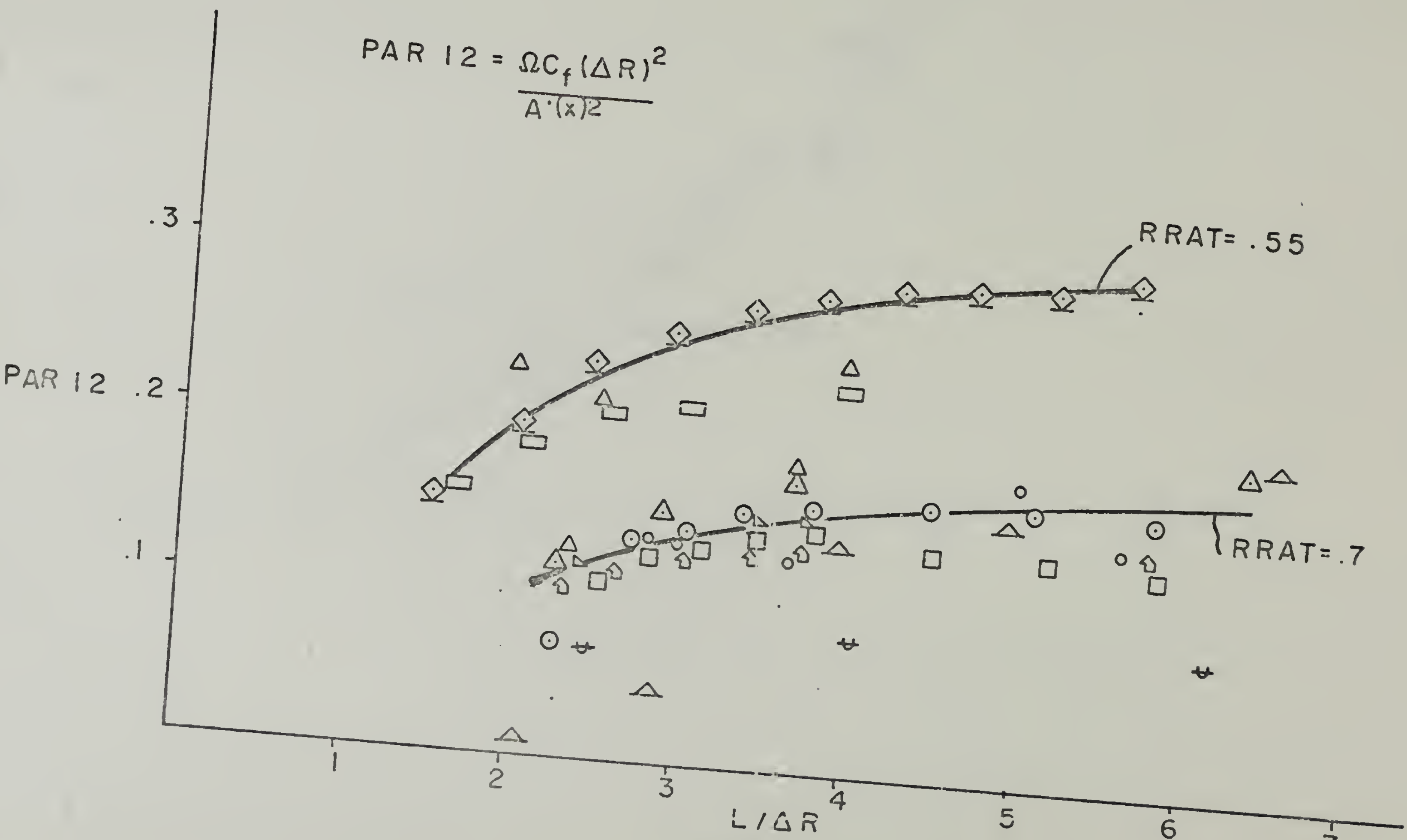
PAR 12 = $\frac{\Omega C_f (\Delta R)^2}{A \cdot (x)^2}$
PAR 12
.3
.2
.1
1
2
3
4
5
6
7
L/ΔR
RRAT= .55
RRAT= .7

FIGURE 13

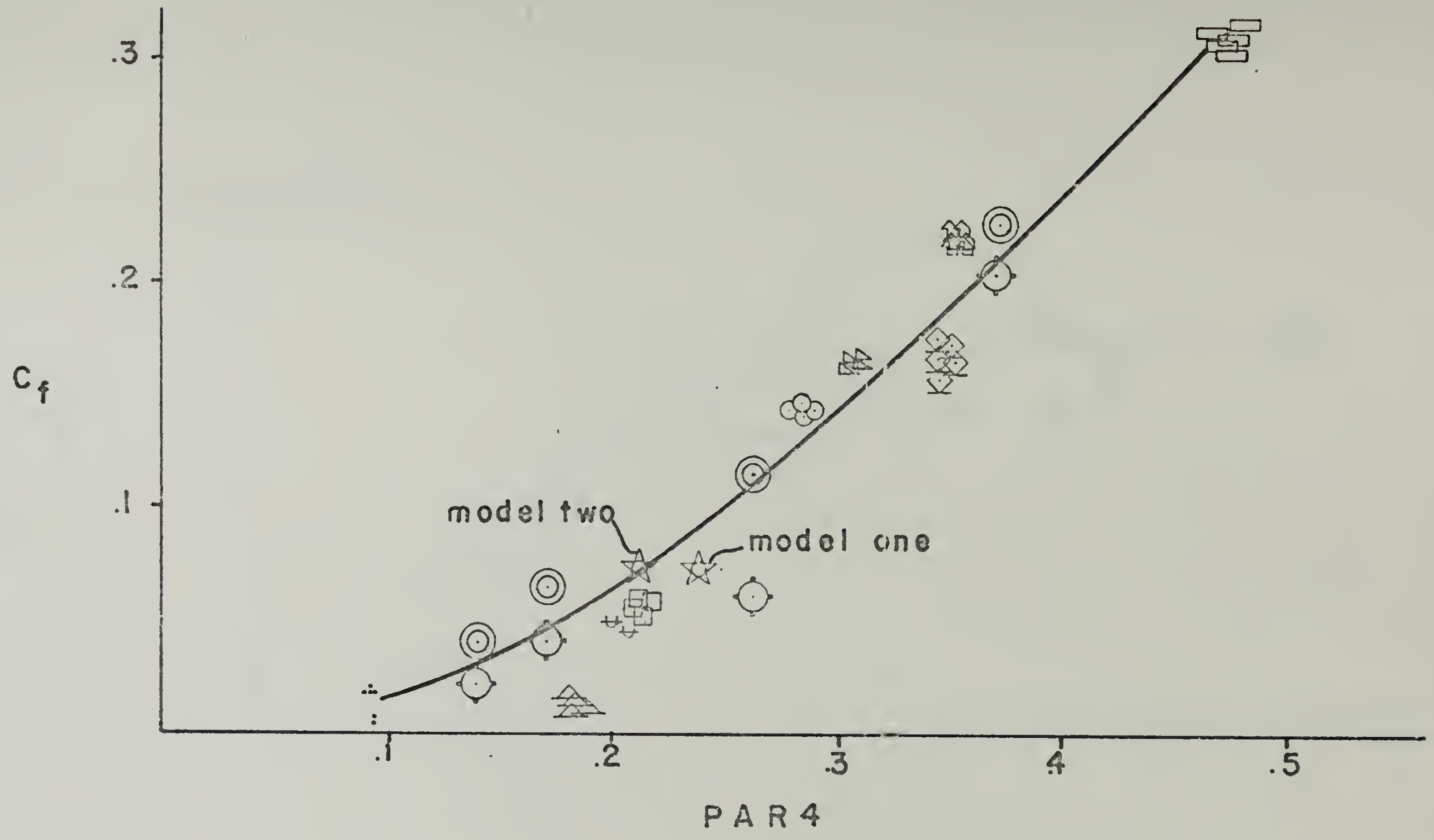

FIGURE 14

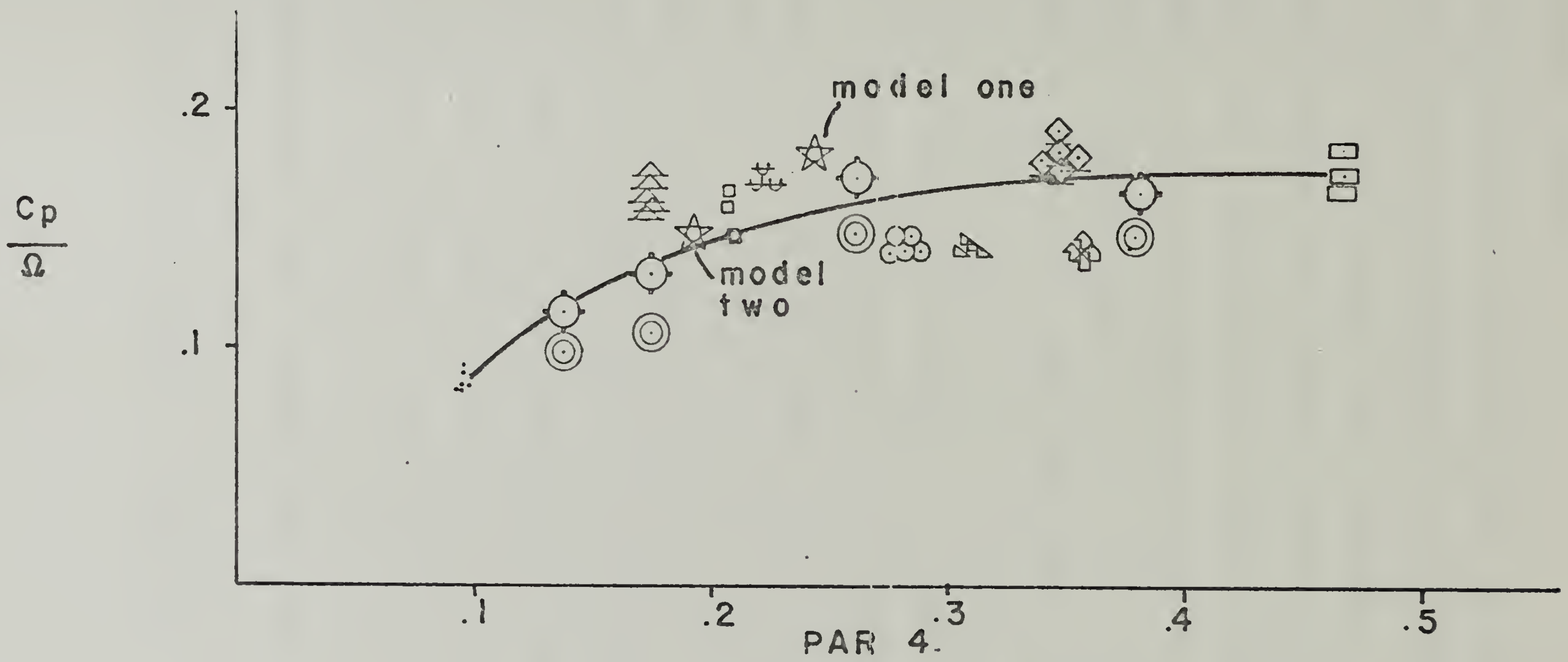

FIGURE 15

# VII. EXPERIMENTAL WORK

## A. EXPERIMENTAL EQUIPMENT

Two annular diffusers were designed and tested in order to provide further data in the evaluation of any trends or correlations discovered from analysis of the literature. The diffusers were designed with the aid of program DESIGN which is listed in the appendix. With a given inner wall angle, fifteen degrees, the program varied the outer wall angle and length to maintain a given area ratio and calculated omega for each case. Both diffusers had an area ratio of three and an inner wall angle of fifteen degrees. Model one had an axial length of 7.73 inches with an outer wall angle of nineteen and one half degrees, and model two had an outer wall angle of eighteen degrees with an axial length of 9.36 inches. Both diffusers had an inlet hub radius, Rhl, of 1.875 inches and an outer inlet radius, Rtl, of 3.123 inches. Model one had an omega of four and model two had an omega of five. Both were constructed from phenolic resin. The above information is summarized in Figure 16. Figure 17 is a photograph of the inner body and model two. In order to supply a uniform flow to the diffusers, a contraction cone was designed by the method described in Ref. 7 and was also fabricated from phenolic resin. Figure 18 is a photograph of the contraction cone and model one. The inner body was supported by three struts mounted in the cone as can be seen from the overall drawing of the assembly in Figure 19.

Static pressure taps were placed at intervals of two inches with each station having three taps one hundred and twenty degrees apart on the inner and outer bodies. Two stations one hundred and twenty degrees apart were also provided one half inch from the inlet plane to made radial surveys. A survey station was also located 8.25 inches upstream from the diffuser inlet station to make cross sectional velocity provile measurements and detailed measurements of the boundary layer. Hot wire anemometer techniques were used for these measurements and the static pressures were read from a manometer board. A United Sensor cobra probe was used to measure the inlet dynamic head and it is shown with the hot wire and model in an overall view of the assembly in Figure 20.

The flow delivery system consisted of an axial compressor, two settling chambers, flow straighteners, and an eight inch pipe. The compressor was an Allis-Chalmers twelve stage axial compressor which operated at a pressure ratio of three to one. After leaving the compressor, the air was cooled and sent through flow straighteners into a large plenum. After passing through a flow straightener the air passed through a sharp edged-orifice for flow measurements. Before being supplied to the eight inch pipe, the air passed through the second plenum. After leaving the eight inch pipe the flow entered the contraction cone and then the model. Meriam micromanometers indicated the pressure readings for flow rate calculations.

B. EXPERIMENTAL RESULTS

Any irregularities in the inlet velocity progile to a diffuser can cause separation and poor performance, therefore it was necessary to insure that the inlet profile was uniform. The hot wire was used to make a survey at the measuring station on the contraction cone to measure the profile and boundary layer thickness. The contraction device provided a uniform inlet flow, as can be seen by the measurements of the velocity distributions at the station 8.25 inches upstream of the diffuser inlet presented in Figure 21. The boundary layer thickness was about .2 inches and the displacement thickness was calculated to be .051 inches and the momentum thickness .014 inches. The flow at the inlet plane of the diffuser is also important. It was checked with a hot wire and the velocity profiles for both models were found to be rather flat as shown in Figure 22. The assurance of uniform inlet flow was important for the possibility of comparing this data with the other existing data. Uncontrolled non-uniformities resulted in flow separation at the diffuser inlet in previous tests with a badly designed contraction device.

The most important result of a diffuser test is the pressure recovery of the models. The static taps allowed a measurement of pressures around the inner and outer bodies and the cobra probe was used to measure the inlet dynamic head. The pressure coefficient is defined as

$$C_p = (P_2 - P_1)/q_1$$

where $P_2$ is taken as atmospheric pressure. Both diffusers had an ideal recovery doefficient of .989. The non-dimensional static

pressure distribution for model one is shown in Figure 23. The recovery and losses are also shown on the graph. Model two also had good recovery as shown in Figure 24. The tests are presented in Figures 14 and 15. It can be seen that they agree with the published data presented in these figures.

$L = 7.73''$ for model one $\quad \alpha_t = 19.5°$ for model one

$L = 9.36''$ for model two $\quad \alpha_t = 18.0°$ for model two

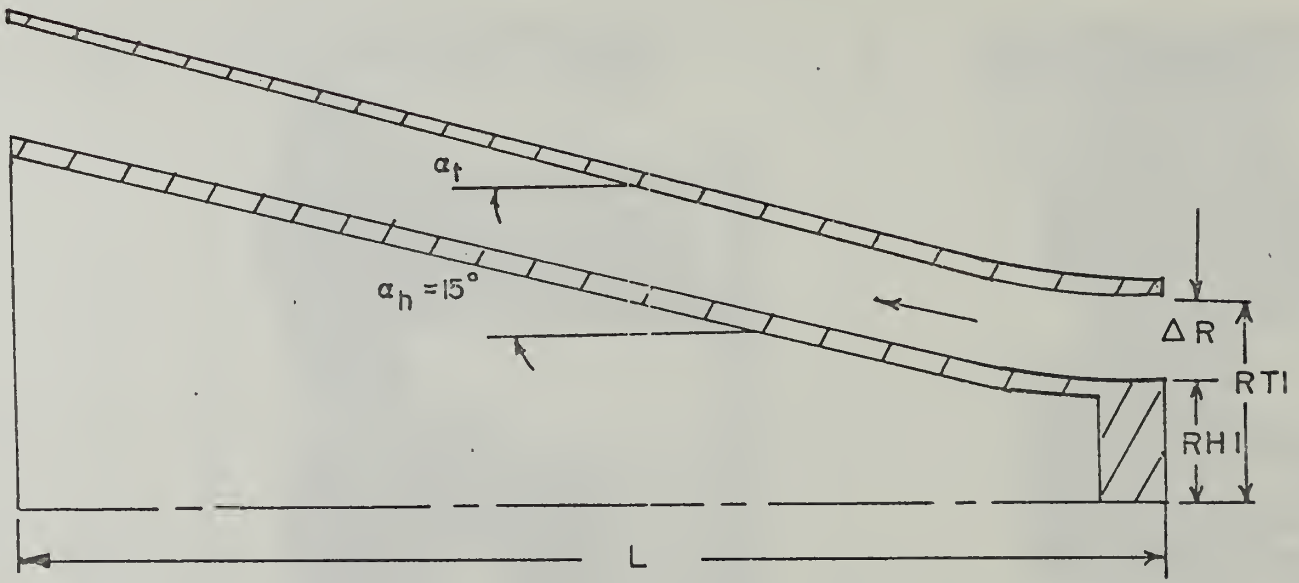

FIGURE 16

MODEL SCHEMATIC

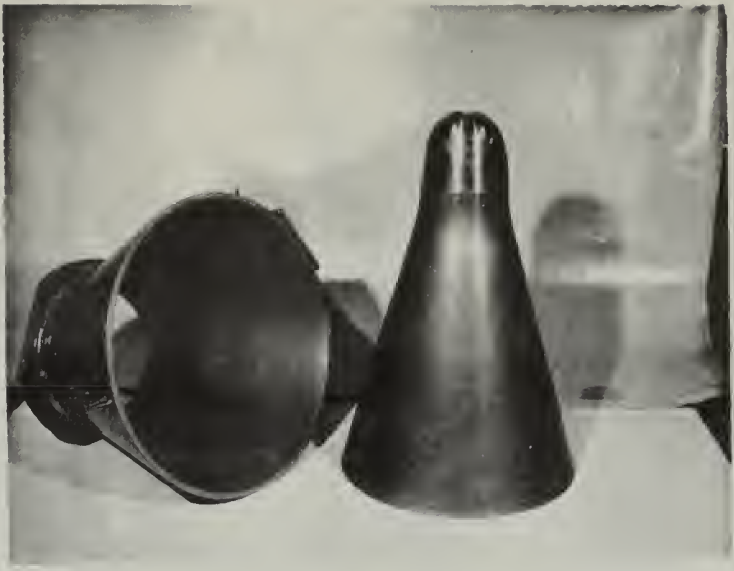

Figure 17 Inner body and model two

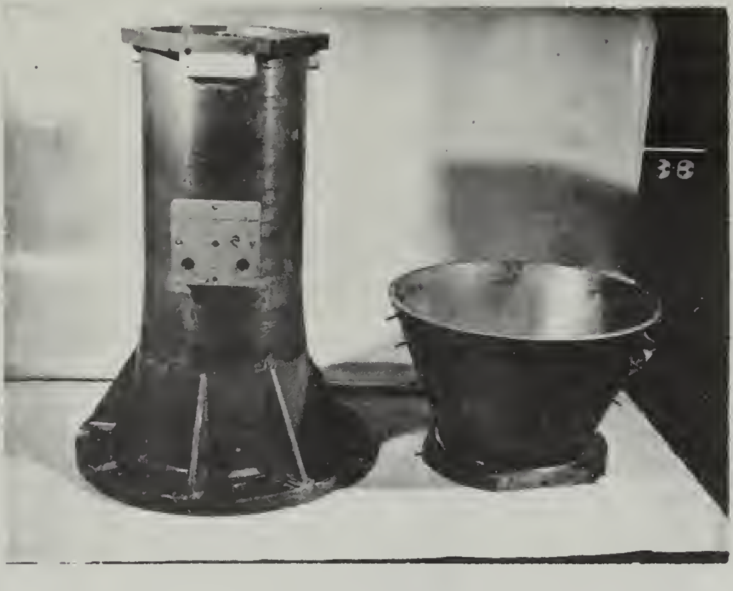

Figure 18 Contraction cone and model one

[illegible]

[illegible]

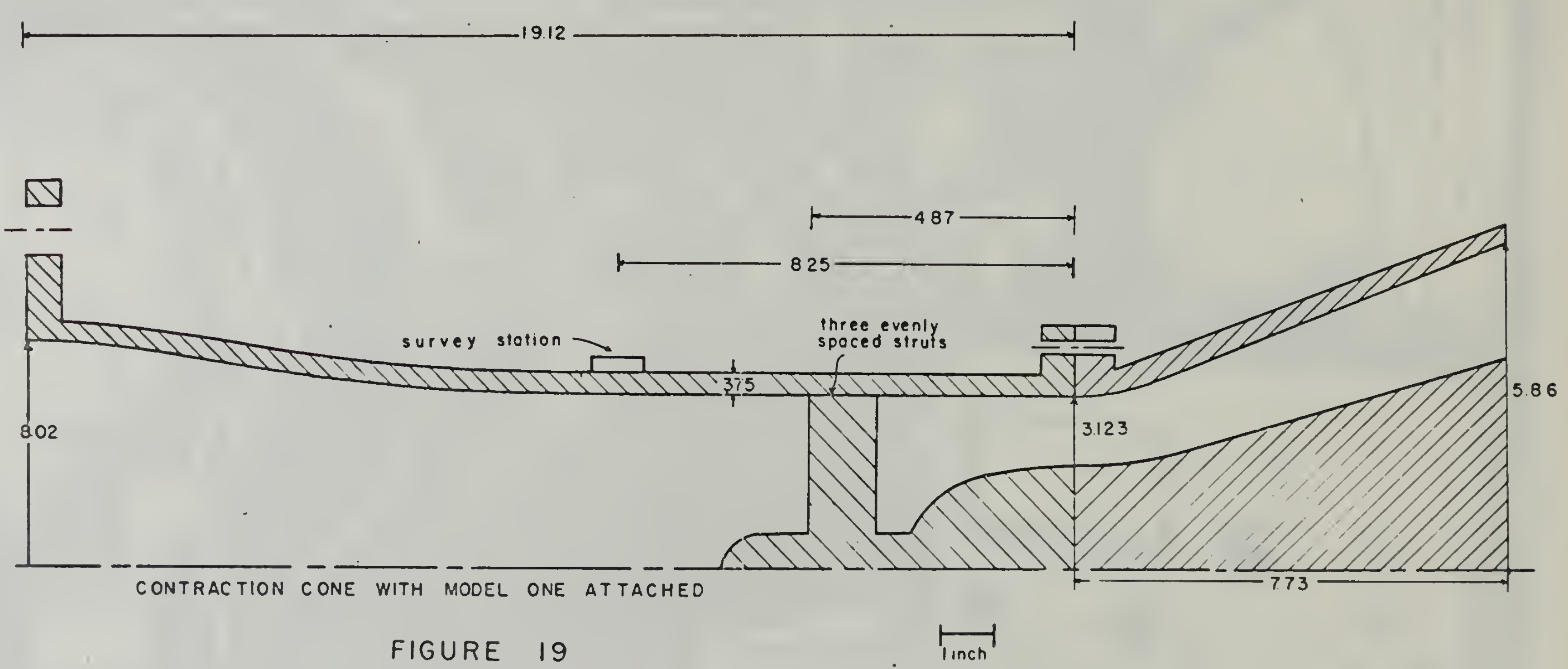

CONTRACTION CONE WITH MODEL ONE ATTACHED

FIGURE 19

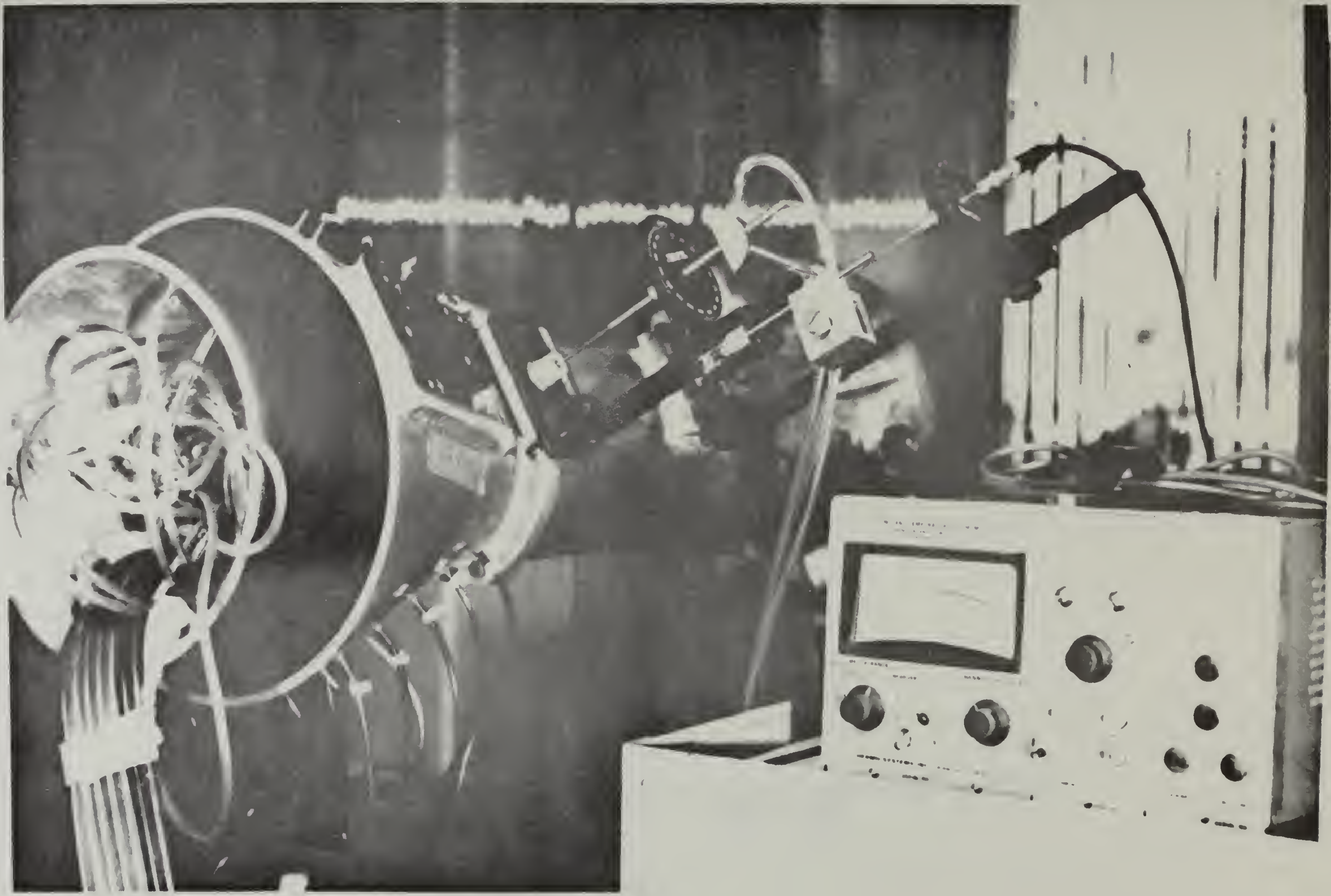

Figure 20  Photograph of equipment

CONTRACTION CONE VELOCITY PROFILE

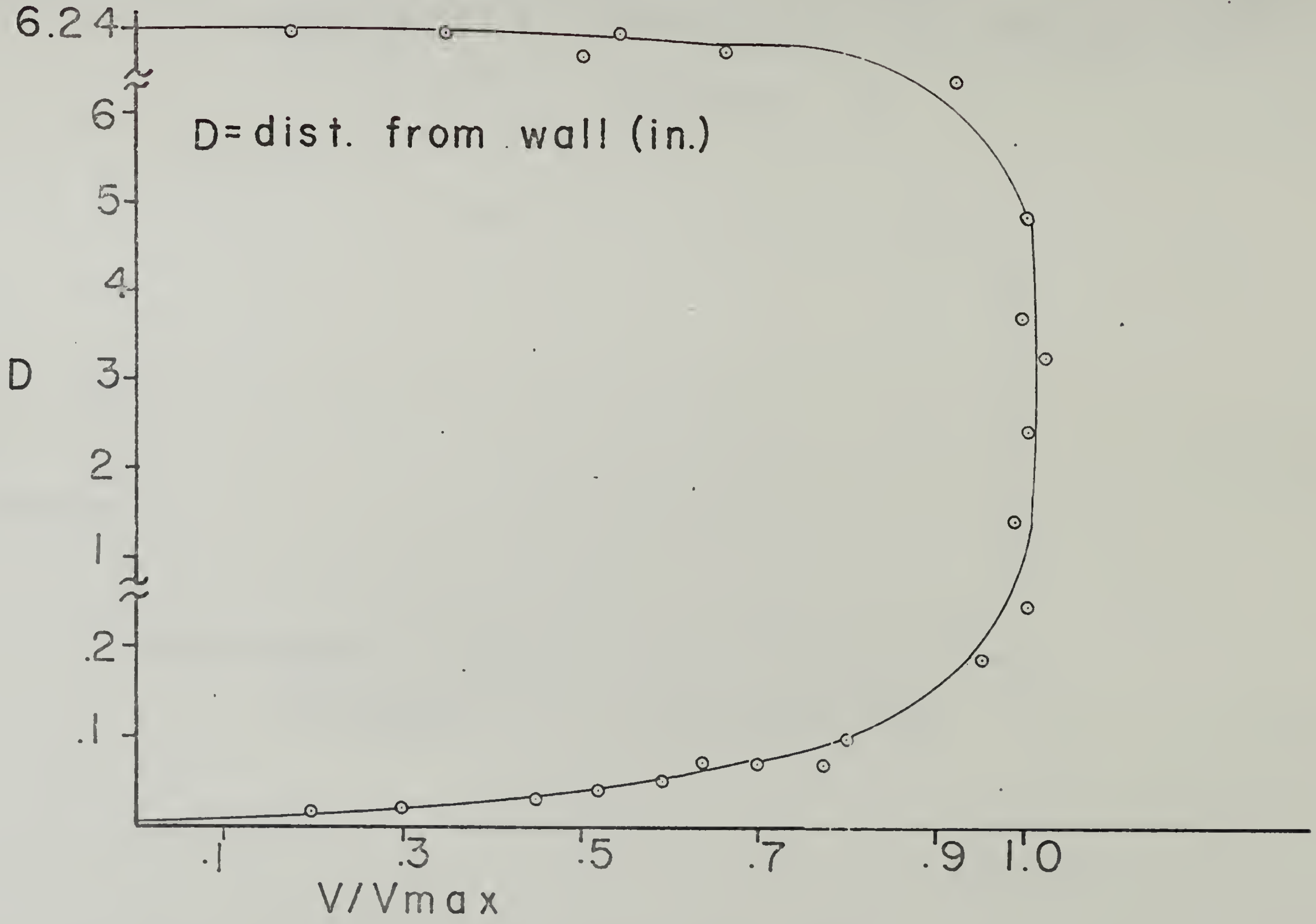

FIGURE 21

VELOCITY PROFILE AT INLET OF
MODEL 2

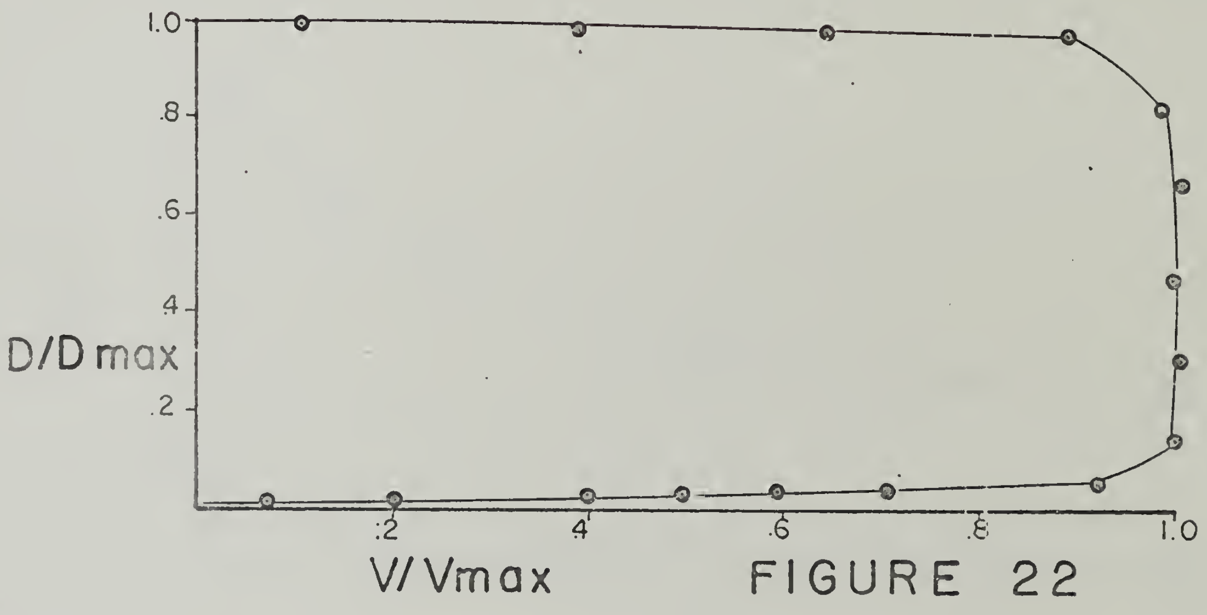

FIGURE 22

MODEL TWO PERFORMANCE

$\dot{m} = 1.87$ lbm/sec
$Rn = 1.12 \times 10^5$
$Cp = .718$

symbols same as fig. 23

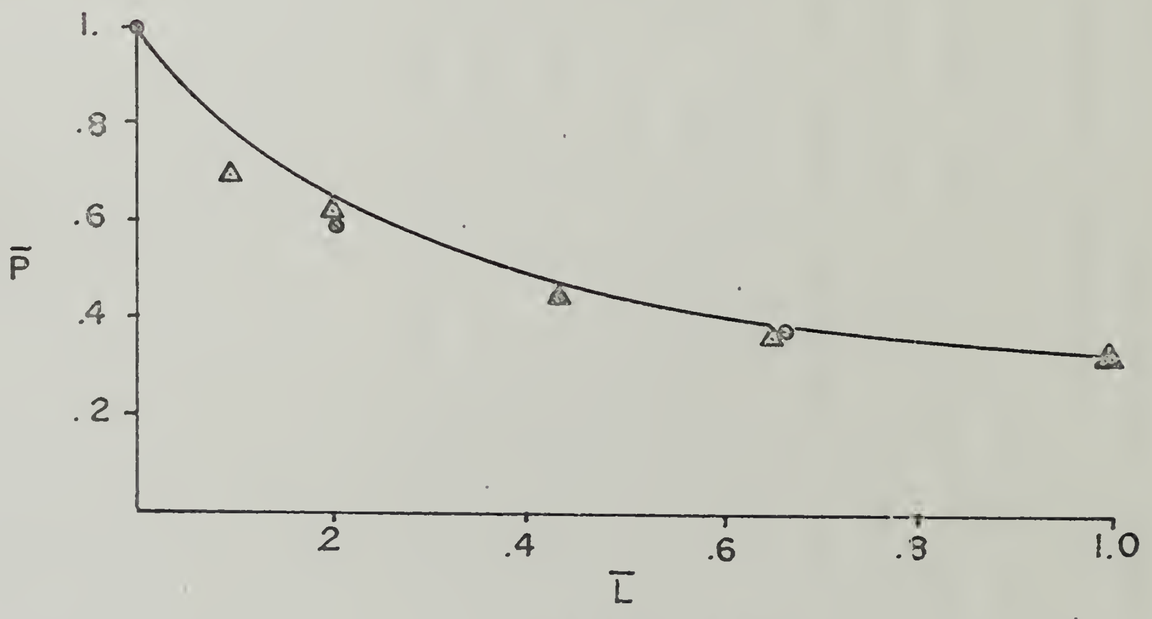

FIGURE 24

# VIII. CONCLUSIONS AND RECOMMENDATIONS

Diffuser performance was investigated in order to obtain a simple correlation to use for design purposes which related diffuser geometry to performance. From analysis of the available experimental data a geometric parameter suggested by Vavra, $\Omega$ (Section II, p. 17), was used to relate the important performance quantities to geometry in a simple manner. A correlation relating the available experimental conical and annular diffuser data was finally established between diffuser geometry and performance without considering the status of the inlet boundary layer. The method of utilization of the correlation in minimizing the diffuser length for a specified pressure recovery, and maximizing recovery for an available length, was also indicated.

Two diffusers were designed and tested to provide additional experimental data and results were found to agree with the developed correlation. More diffusers should be designed and tested in the region of the correlation where the data are not plentiful. The influence of the inlet boundary layer and Reynolds number must be investigated, since it is felt that these two factors are among the causes of the scatter in the derived correlation.

# APPENDIX A

Program Design was formulated to aid in the design of the diffusers mentioned in the experimental section. The purpose of the program was to vary the outer wall angle from sixteen to twenty-two degrees in increments of one quarter while always maintaining a specified area ratio. This procedure was done for three different area ratios. The program calculated omega for each wall angle combination by the use of a numerical integration scheme which employed an external function.

### List of Symbols

A1 - inlet area
A2 - outlet area
A - area
C - circumference
I - logical control variable
RH1 - inlet inner radius
RT1 - inlet outer radius
AHR - inner wall angle in radians
ATR - outer wall angle in radians
RT2 - outlet outer radius
RH2 - outlet inner radius
XU - upper limit on omega integration
XL - lower limit on omega integration
A5 - (A1/A)**3
A6 - 2*(C/A1)
Y - omega

## Parameter Study Programs

There were three programs to complete the parameter study, and the program of each diffuser type is basically the same. The same integration scheme was used to calculate omega as the pertinent parameters were varied. PARSTUDY 1 was for annular diffusers, PARSTUDY2 for two dimensional and PARSTUDY3 for conical diffusers. The main device used was a set of nested do loops and the variables in these programs were identical to those in the previous programs except as follows.

### PARSTUDY1

ALFAH - inner wall angle
ALFAT - outer wall angle
LDELR - dimensionless length
TAT - tangent of outer wall angle
TAH - tangent of inner wall angle
DELR - difference between inner and outer inlet radius

### PARSTUDY2

LW1 - non dimensional length
B1 - inlet dimension
W1 - inlet dimension

### PARSTUDY3

R - inlet radius
LR - non dimensional length

Program DATA was the most extensively used program in the thesis and allowed the determination of all necessary numerical parameters for the annular diffuser data of Sovran and Klomp. The numerical integration scheme was used in this program to calculate omega, and the same symbols in the external function

were used as in DESIGN. The data was read from data cards and the parameters listed in the table of symbols were calculated.

List of Symbols

FAM - diffuser wall angle combination (family of Sovran and Klomp)
AT - outer wall angle
AH - inner wall angle
RRAT - inlet radius ratio
DIML - dimensionless length
AR - area ratio
CPI - ideal recovery coefficient
CP - pressure recovery coefficient
I - logical control variable
OCF - $\Omega C_f$
RT1 - inlet outer radius
RH1 - inlet inner radius
DADX - area gradient
BARL - diffuser length
Y - omega
RM - mean radius
A1 - inlet area

```
C                                   DESIGN




      EXTERNAL FCT
      REAL*4 L
      I=0
      RT1=3.123
      RH1=1.875
      A2=40.0
      AHR=15./57.3
 1    AT=16.
 2    ATR=AT/57.3
      TATR=SIN(ATR)/COS(ATR)
      TAHR=SIN(AHR)/COS(AHR)
      C=TATR/TAHR
      D=RT1-RH1*C
      C2=D**2-A2/3.141
      B=2*D*C
      A=C**2-1.
      B3=B**2-4.*A*C2
10    RH2=(-B+B3**.5)/(2.*A)
      DIFL=(RH2-RH1)/TAHR
      RT2=(A2/3.141+RH2**2)**.5
      R=DIFL/COS(ATR)
      BIGL=(R+DIFL)/2.
C   START NUMERICAL INTEGRATION ROUTINE
      XU=BIGL
      XL=0
      A=.5*(XU+XL)
       D=XU-XL
      C=.4840801*D
      Y=.04663719*(FCT(A+C,TATR,TATR)+FCT(A-C,TATR,TAHR))
       C=.4180156*D
      Y=Y+.0903248*(FCT(A+C,TATR,TAHR)+FCT(A-C,TATR,TAHR))
        C=.3066857*D
      Y=Y+.1303053*(FCT(A+C,TATR,TAHR)+FCT(A-C,TATR,TAHR))
       C=.1621267*D
      Y=Y+.1561735*(FCT(A+C,TATR,TAHR)+FCT(A-C,TATR,TAHR))
      Y=D*(Y+.1651197*FCT(A, TATR,TAHR))
C   END INTEGRATION
      WRITE(6,3)Y,AT,RT2,RH2,DIFL
3     FORMAT(' ','OMEGA=',F5.2,2X,'ALPHA=',F5.2,2X,'RT2=',F4
     1.2,2X,'RH2=',F4.2,2X,'DIFL=',F5.2)
      AT=AT+.25
      IF(AT.GT.22.0) GO TO 4
      GO TO 2
4     I=I+1.
      WRITE(6,11)
11    FORMAT(///,20X,'NEW AREA RATIO',///)
      IF(I.EQ.1.) GO TO 6
      IF(I.EQ.2.) GO TO 5
      IF (I.EQ.3) GO TO 7
5     A2=50.0
      GO TO 1
6     A2=68.5
      GO TO 1
7     STOP
      END

      FUNCTION FCT(X,TATR,TAHR)
      RT1=3.123
      RH1=1.875
      X1=RT1**2-RH1**2.
      X2=(RT1+X*TATR)**2.
      X3=(RH1+X*TAHR)**2.
      A5=(X1/(X2-X3))**3.
      A6=2.*((X2**.5)+(X3**.5))/X1
      FCT=A5*A6
      RETURN
      END
//GO.SYSIN DD *
```

```
C                   CONICAL PARAMETER STUDY
C                   PARSTUDY1
//
//
//
```

```
      IMPLICIT REAL*4(L)
      EXTERNAL FCT
      WRITE(6,17)
17    FORMAT('1')
      A1=1.
      R=(1./3.141)**.5
      ALFA=1.
      LR=1.
      DO1 I=1,15
      DO 2 J=1,15
      ALFAR=ALFA/57.3
      TAN=SIN(ALFAR)/COS(ALFAR)
      XU=LR*R
      AR=3.141*(R+XU*TAN)**2
      CPI=1.-1./AR**2
      XL=0.0
      A=.5*(XU+XL)
      D=XU-XL
      C=.4840801*D
      Y=.04063719*(FCT(A+C,TAN)+FCT(A-C,TAN))
      C=.4180156*D
      Y=Y+.1303053*(FCT(A+C,TAN)+FCT(A-C,TAN))
      C=.3066857*D
      Y=Y+.09032408*(FCT(A+C,TAN)+FCT(A-C,TAN))
      C=.1621267*D
      Y=Y+.1561735*(FCT(A+C,TAN)+FCT(A-C,TAN))
      Y=D*(Y+.1651197*FCT(A,TAN))
      WRITE(6,3)Y,LR,ALFA,R
3     FORMAT(' OMEGA=',F5.2,2X,'L/R=',F5.2,2X,'ALFA=',F5.2,2
     1X,'R=',F4.3)
      ALFA=ALFA+1.0
 2    CONTINUE
      ALFA=1.0
      LR=LR+1.0
1     CONTINUE
      STOP
      END

      FUNCTION FCT(X,TAN)
      A1=1.
      R=(1./3.141)**.5
      A=3.141*(R+X*TAN)**2
      X1=(A1/A)**3
      C=2.*3.141*(R+X*TAN)
      X2=C/A1
      FCT=X1*X2
      RETURN
      END
//GO.SYSIN DD *
```

```
C                    TWO DIMENSIONAL PARAMETER STUDY
C                    PARSTUDY2




      IMPLICIT REAL*4(L)
      EXTERNAL FCT
      ALFA=0.0
      A1=1.0
      LW1=1.0
      B1=1.
      DO 1 M=1,7
      DO 2 N=1,7
      DO 3 I=1,6
      ALFAR=ALFA/57.3
      TAN=SIN(ALFAR)/COS(ALFAR)
      W1=1./B1
      L=LW1*W1
      AR=A1+2.*L*TAN*B1
      CPI=1.-1./AR**2
      XU=L
      XL=0.0
      A=.5*(XU+XL)
      D=XU-XL
      C=.4840801*D
      Y=.04063719*(FCT(A+C,TAN,B1,W1)+FCT(A-C,TAN,B1,W1))
      C=.4180156*D
      Y=Y+.1303053*(FCT(A+C,TAN,B1,W1)+FCT(A-C,TAN,B1,W1))
      C=.3066857*D
      Y=Y+.0903243*(FCT(A+C,TAN,B1,W1)+FCT(A-C,TAN,B1,W1))
      C=.1621267*D
      Y=Y+.1561735*(FCT(A+C,TAN,B1,W1)+FCT(A-C,TAN,B1,W1))
      Y=D*(Y+.1651197*FCT(A,TAN,B1,W1))
      WRITE(6,4)Y,LW1,W1,B1,ALFA
4     FORMAT(' OMEGA=',F5.2,2X,'L/W1=',F5.2,2X,'W1=',F5.2,2X
     1,'B1=',F4.2,2X,'ALFA=',F4.1)
      B1=B1+1.
3     CONTINUE
      B1=1.
      ALFA=ALFA+2.0
2     CONTINUE
      B1=1.
      ALFA=1.0
      LW1=LW1+2.
1     CONTINUE
      STOP
      END

      FUNCTION FCT(X,TAN,B1,W1)
      A1=1.
      A=A1+2.*X*TAN*B1
      X1=(A1/A)**3
      C=2.*W1+2.*B1+4.*X*TAN
      X2=C/A1
      FCT=X1*X2
      RETURN
      END
//GO.SYSIN DD *
```

```
C                      ANNULAR PARAMETER STUDY
C                             PARSTUDY3




      IMPLICIT REAL*4(L)
      EXTERNAL FCT
      WRITE(6,25)
25    FORMAT('1')
      A1=20.
      ALFAH=0.0
      ALFAT=1.0/57.3
      LDELR=1.0
      RI=2.0
      DO 1 M=1,7
      DO 2 J=1,21,5
      N=J+1
      DO 3 K=N,22,5
      DO 4 I=1,4
      RO=(A1/3.141+RI**2)**.5
      DELR=RO-RI
      ALFATR=ALFAT*57.3
      ALFAHR=ALFAH*57.3
      TAT=SIN(ALFAT)/COS(ALFAT)
      TAH=SIN(ALFAH)/COS(ALFAH)
      XU=LDELR*DELR
      AR=(3.141*((RO+XU*TAT)**2-(RI+XU*TAH)**2))/A1
      CPI=1.-(1./AR)**2
      DADX=2.*RO*TAT-2.*RI*TAH
      DIFF=((TAT)**2-(TAH)**2)*2.
      XL=0.0
      A=.5*(XU+XL)
      D=XU-XL
      C=.4840801*D
      Y=.04063719*(FCT(A+C,RI,RO,TAT,TAH)+FCT(A-C,RI,RO,TAT,
     1TAH))
      C=.4180156*D
      Y=Y+.09032408*(FCT(A+C,RI,RO,TAT,TAH)+FCT(A-C,RI,RO,TA
     1T,TAH))
      C=.3066857*D
      Y=Y+.1303053*(FCT(A+C,RI,RO,TAT,TAH)+FCT(A-C,RI,RO,TAT
     1,TAH))
      C=.1621267*D
      Y=Y+.1561735*(FCT(A+C,RI,RO,TAT,TAH)+FCT(A-C,RI,RO,TAT
     1,TAH))
      Y=D*(Y+.1651197*FCT(A,RI,RO,TAT,TAH))
      WRITE(6,5)Y,LDELR,DADX
5     FORMAT(' ','OMEGA=',F5.2,3X,'LDELR=',F6.2,3X,'DADX=',
     1F5.2)
      RI=RI+2.0
4     CONTINUE
      RI=2.0
      ALFAT=ALFAT+5./57.3
3     CONTINUE
      RI=2.0                                FUNCTION FCT(X,RI,RO,TAT,TAH)
      ALFAH=ALFAH+5./57.3                   A1=20.
      ALFAT=ALFAH+1./57.3                   X2=(RO+X*TAT)**2
2     CONTINUE                              X1=(RI+X*TAH)**2
      RI=2.0                                A3=3.141*(X2-X1)
      ALFAH=0.0                             X3=(A1**2)/(A3**2)
      ALFAT=1.0/57.3                        X4=2.*3.141*((X1**.5)+(X2**.5))
      LDELR=LDELR+2.                        FCT=X3*X4
1     CONTINUE                              RETURN
      STOP                                  END
      END                                 .SYSIN DD *
```

```
C                        DATA REDUCTION FROM SOVRAN AND KLOMP





      EXTERNAL FCT
      REAL*4 L
      RT1=7.55
      WRITE(6,45)
45    FORMAT('1')
 1    READ(5,10) FAM,AT,AH,RRAT,DIML,AR,CPI,CP,I
 10   FORMAT(3F5.2,F3.2,F5.2,F5.3,2F4.3,I1)
      DCF=CPI-CP
      RH1=RT1*RRAT
      DELR=RT1-RH1
      ATR=AT/57.3
      AHR=AH/57.3
      TATR=SIN(ATR)/COS(ATR)
      TAHR=SIN(AHR)/COS(AHR)
      DADX=2.*(RT1*TATR-RH1*TAHR)
      BARL=DIML*(RT1-RH1)
      XU=BARL
      XL=0.0
      A=.5*(XU+XL)
       D=XU-XL
      C=.4840801*D
       Y=.04063719*(FCT(A+C,ATR,AHR,RH1)+FCT(A-C,ATR,AHR,RH
     1))
       C=.4130156*D
       Y=Y+.09032408*(FCT(A+C,ATR,AHR,RH1)+FCT(A-C,ATR,AHR,R
     1H1))
        C=.3066857*D
       Y=Y+.1303053*(FCT(A+C,ATR,AHR,RH1)+FCT(A-C,ATR,AHR,RH
     11))
       C=.1621267*D
       Y=Y+.1561735*(FCT(A+C,ATR,AHR,RH1))
       Y=D*(Y+.1651197*FCT(A,ATR,AHR,RH1))
      PAR1=(DADX-1.5)/DELR
      PAR11=DCF/PAR1
      PAR2=(DADX/DELR)**2.
      PAR21=DCF/PAR2
      PAR4A=2*(TATR-RRAT*TAHR)/(1.+RRAT)
      PAR5=(CP/CPI)*PAR4A
      CF=PAR4A*(1.-CP/CPI)
      WRITE(6,99)FAM,PAR4A,CF,PAR5,Y
99    FORMAT(' ','FAM=',F5.2,3X,'PAR4A=',E10.3,3X,'CF=',E10
     1.3,3X,'CP/OMEGA=',E10.3,3X,'OMEGA=',F5.2)
      WRITE(6,77)
77    FORMAT(/)
      IF(I.EQ.1) GO TO 4
      GO TO 6
4     WRITE(6,7)
7     FORMAT(///,20X,'NEW FAMILY',///)
6     IF(I.EQ.2) GO TO 8
      GO TO 1
8     STOP
      END


      FUNCTION FCT(X,ATR,AHR,RH1)
      RT1=7.55
      X1=RT1**2-RH1**2.
       TATR=SIN(ATR)/COS(ATR)
       TAHR=SIN(AHR)/COS(AHR)
      X2=(RT1+X*TATR)**2.
      X3=(RH1+X*TAHR)**2.
      AS=(X1/(X2-X3))**3.
```

```
      A6=2.*((X2**.5)+(X3**.5))/X1
      FCT=A5*A6
      RETURN
      END
//GO.SYSIN DD *
15.1515.0015.00.7002.281.167.266.2560
15.1515.0015.00.7003.631.286.396.3670
15.1515.0015.00.7005.661.465.534.4500
15.1515.0015.00.7008.371.704.656.5410
15.1515.0015.00.7009.721.823.699.5640
15.1515.0015.00.7011.071.943.735.5890
15.1515.0015.00.7013.102.122.778.6261
20.1520.0015.00.7003.051.613.615.4420
20.1520.0015.00.7003.401.699.653.4680
20.1520.0015.00.7003.751.787.687.4920
20.1520.0015.00.7004.441.971.743.5560
20.1520.0015.00.7005.142.163.786.6030
20.1520.0015.00.7005.832.365.821.6441
20.1020.0010.00.7002.341.660.637.3140
20.1020.0010.00.7002.681.779.684.3350
20.1020.0010.00.7003.031.902.723.3490
20.1020.0010.00.7003.382.028.757.3620
20.1020.0010.00.7003.732.158.785.3690
20.1020.0010.00.7004.422.430.831.4030
20.1020.0010.00.7005.122.717.865.4340
20.1020.0010.00.7005.802.965.886.4591
20.0820.0008.25.7002.331.730.666.2990
20.0820.0008.25.7002.681.860.711.3150
20.0820.0008.25.7003.031.995.749.3310
20.0820.0008.25.7003.372.133.780.3420
20.0820.0008.25.7003.722.276.807.3541
20.0520.0005.00.7002.321.851.708.2760
20.0520.0005.00.7002.662.001.750.2840
20.0520.0005.00.7003.012.156.785.2930
20.0520.0005.00.7003.362.316.814.2990
20.0520.0005.00.7003.712.481.838.3070
20.0520.0005.00.7005.793.569.921.3491
30.2930.0029.50.7002.421.265.375.2760
30.2930.0029.50.7003.921.521.568.4530
30.2930.0029.50.7006.111.907.725.6060
30.2930.0029.50.7009.172.471.836.7191
05.0005.0000.00.5501.471.169.268.3050
05.0005.0000.00.5502.341.274.384.4030
05.0005.0000.00.5503.641.437.516.5210
05.0005.0000.00.5505.381.668.641.6201
15.0015.0000.00.5501.501.531.574.3520
15.0015.0000.00.5501.951.713.659.3620
15.0015.0000.00.5502.401.902.723.3850
15.0015.0000.00.5502.852.099.773.4030
15.0015.0000.00.5503.302.304.812.4210
15.0015.0000.00.5503.752.517.842.4380
15.0015.0000.00.5504.202.738.867.4480
15.0015.0000.00.5504.662.967.886.4620
15.0015.0000.00.5505.113.205.903.4710
15.0015.0000.00.5505.553.450.916.4771
15.1315.0013.50.5502.011.314.421.4150
15.1315.0013.50.5502.861.462.532.5160
15.1315.0013.50.5503.811.650.633.5870
15.1315.0013.50.5504.711.827.701.6430
15.1315.0013.50.5506.522.200.793.7200
15.1315.0013.50.5508.312.595.851.7811
20.0020.0000.00.5501.561.570.673.2590
20.0020.0000.00.5502.022.012.753.2710
20.0020.0000.00.5502.492.289.809.2810
20.0020.0000.00.5502.952.581.850.2980
20.0020.0000.00.5503.422.888.880.2960
20.0020.0000.00.5503.883.209.903.3041
20.1320.0013.50.5502.081.603.611.3620
20.1320.0013.50.5502.541.770.681.4760
20.1320.0013.50.5503.032.320.814.5562
15.1515.0015.00.7005.661.465.534.4500
15.1515.0015.00.7008.371.704.656.5410
```

# BIBLIOGRAPHY

1. Cocanower, A. B., Kline, S. J., and Johnston, J. P., "A Unified Method for Predicting the Performance of Subsonic Diffusers of Several Geometries," Report PD-10, Thermosciences Division, Mechanical Engineering Department, Stanford University, May 1965.

2. Cockrell, D. J. and Markland, E., "A Review of Incompressible Diffuser Flow," Aircraft Engineering, v. 35, pp. 288-292, October 1963.

3. Gapp, D. R., A Design Criterion for Arbitrary Diffusers, Aeronautical Engineer Thesis, U.S. Naval Postgraduate School, Monterey, California, June 1970

4. Gleason, J. G., An Investigation of Current Subsonic Diffuser Design Knowledge with Emphasis on Jet Engine Annular Diffusers, A Pratt and Whitney Summer Faculty Program Project, Summer 1963.

5. Reneau, L. R., Johnston, J. P., and Kline, S. J., "Performance and Design of Straight, Two Dimensional Diffusers," Report PD-8, Thermosciences Division, Mechanical Engineering Department, Stanford university, September 1964.

6. Sovran, G. and Klomp, D. D., Experimentally Determined Optimum Geometries for Rectilinear Diffusers with Rectangular Conical or Annular Cross-Section, Engineering Development Department Research Laboratories, General Motors Corporation, Warren, Michigan, 16 November 1965.

7. Tsien, H. "On the Design of a Contraction Cone for a Wind Tunnel, "Journal of Aeronautical Sciences, pp. 68-70, February 1943.

8. Vavra, M. H., Agard Lecture Series 39, Lecture Series on Basic Elements for Advanced Designs of Radial-Flow Compressors, June 1970.

# INITIAL DISTRIBUTION LIST

| | | No. Copies |
|---|---|---|
| 1. | Defense Documentation Center<br>Cameron Station<br>Alexandria, Virginia 22314 | 2 |
| 2. | Library, Code 0212<br>Naval Postgraduate School<br>Monterey, California 93940 | 2 |
| 3. | Chairman, Department of Aeronautics<br>Naval Postgraduate School<br>Monterey, California 93940 | 1 |
| 4. | Kyriacos Papailiou (thesis advisor)<br>Dip. Mech. Eng., Dip. Aero.<br>von Karman Institute<br>72, Chaussee De Waterloo<br>Rhode-Saint-Genese<br>Belgium | 1 |
| 5. | Professor M. H. Vavra<br>Department of Aeronautics<br>Naval Postgraduate School<br>Monterey, California 93940 | 5 |
| 6. | K. W. Sharer<br>6015 Lamont Court<br>Springfield, Virginia 22152 | 1 |

## DOCUMENT CONTROL DATA - R & D

(Security classification of title, body of abstract and indexing annotation must be entered when the overall report is classified)

| | | |
|---|---|---|
| 1. ORIGINATING ACTIVITY (Corporate author)<br>Naval Postgraduate School<br>Monterey, California 93940 | 2a. REPORT SECURITY CLASSIFICATION<br>Unclassified<br>2b. GROUP | |
| 3. REPORT TITLE<br>An Investigation of Subsonic Diffuser Performance | | |
| 4. DESCRIPTIVE NOTES (Type of report and, inclusive dates) | | |
| 5. AUTHOR(S) (First name, middle initial, last name)<br>Kevin Woods Sharer | | |
| 6. REPORT DATE<br>June 1971 | 7a. TOTAL NO. OF PAGES<br>81 | 7b. NO. OF REFS<br>8 |
| 8a. CONTRACT OR GRANT NO.<br>b. PROJECT NO.<br>c.<br>d. | 9a. ORIGINATOR'S REPORT NUMBER(S)<br>9b. OTHER REPORT NO(S) (Any other numbers that may be assigned this report) | |
| 10. DISTRIBUTION STATEMENT<br>Approved for public release; distribution unlimited. | | |
| 11. SUPPLEMENTARY NOTES | 12. SPONSORING MILITARY ACTIVITY<br>Naval Postgraduate School<br>Monterey, California 93940 | |

13. ABSTRACT

This report investigates subsonic diffuser performance, with emphasis on conical and annular geometries. A correlation is presented which aids in the prediction of performance. Two annular diffusers were designed and tested to help substantiate the correlation.

| 4 KEY WORDS | LINK A | | LINK B | | LINK C | |
|---|---|---|---|---|---|---|
| | ROLE | WT | ROLE | WT | ROLE | WT |
| anular diffuser<br>dffuser<br>dffuser performance<br>sape parameter<br>cnical diffuser<br>crrelation for diffusers | | | | | | |

DD FORM 1 NOV 65 1473 (BACK)

N 0101-807-6821

9 DEC 71 S10675
10 DEC 72 19885

Thesis 128406
S4345 Sharer
c.1 An investigation of
subsonic diffuser performance.

9 DEC 71 S10675
10 DEC 72 19885

f
r-

Thesis 128406
S4345 Sharer
c.1 An investigation of
subsonic diffuser performance.

thesS4345
An investigation of subsonic diffuser pe
3 2768 001 94372 3
DUDLEY KNOX LIBRARY